doi:10.1111/evo.14629

Cranial ecomorphology of turtles and neck retraction as a possible trigger of ecological diversification

Guilherme Hermanson,[1,2,3,4] Roger B. J. Benson,[2] Bruna M. Farina,[3,5] Gabriel S. Ferreira,[6,7] Max C. Langer,[3] and Serjoscha W. Evers[1]

[1]*Department of Geosciences, University of Fribourg, Fribourg CH-1700, Switzerland*

[2]*Department of Earth Sciences, University of Oxford, Oxford OX1 3AN, United Kingdom*

[3]*Laboratório de Paleontologia de Ribeirão Preto, Universidade de São Paulo, Ribeirão Preto 14040-091, Brazil*

[4]*E-mail: guilhermehermanson@gmail.com*

[5]*Department of Biology, University of Fribourg, Fribourg CH-1700, Switzerland*

[6]*Senckenberg Centre for Human Evolution and Palaeoenvironment (HEP), Eberhard Karls Universität Tübingen 72076, Tübingen, Germany*

[7]*Fachbereich Geowissenschaften, Universität Tübingen 72074, Tübingen, Germany*

Received January 10, 2022
Accepted August 29, 2022

Turtles have a highly modified body plan, including a rigid shell that constrains postcranial anatomy. Skull morphology and neck mobility may therefore be key to ecological specialization in turtles. However, the ecological signal of turtle skull morphologies has not been rigorously evaluated, leaving uncertainties about the roles of ecological adaptation and convergence. We evaluate turtle cranial ecomorphology using three-dimensional geometric morphometrics and phylogenetic comparative methods. Skull shape correlates with allometry, neck retraction capability, and different aquatic feeding ecologies. We find that ecological variables influence skull shape only, whereas a key functional variable (the capacity for neck retraction) influences both shape and size. Ecology and functional predictions from three-dimensional shape are validated by high success rates for extant species, outperforming previous two-dimensional approaches. We use this to infer ecological and functional traits of extinct species. Neck retraction evolved among crownward stem-turtles by the Late Jurassic, signaling functional decoupling of the skull and neck from the shell, possibly linked to a major episode of ecomorphological diversification. We also find strong evidence for convergent ecological adaptations among marine groups. This includes parallel loss of neck retraction, evidence for active hunting, possible grazing, and suction feeding in extinct marine groups. Our large-scale assessment of dietary and functional adaptation throughout turtle evolution reveals the timing and origin of their distinct ecomorphologies, and highlights the potential for ecology and function to have distinct effects on skull form.

KEY WORDS: Cranial shape, ecomorphology, neck retraction, paleontology, turtles.

Fully shelled turtles (Testudinata) are among the three major living reptile groups (alongside lepidosaurs and archosaurs), and have persisted through ~230 million years since their appearance during the Late Triassic (Gaffney 1990; Joyce 2017). Compared to squamates and birds with approximately 10,000 living species each (Jetz et al. 2012; Pincheira-Donoso et al. 2013), turtles are notably species poor, with only 357 extant taxa (Rhodin et al. 2021). Despite this low richness, turtles evolved high ecological diversity, inhabiting distinct habitats spanning arid desert environments, all types of freshwater aquatic settings, and the oceans, with dietary ecologies that range from generalistic omnivory, to highly specialized diets such as high-fiber

herbivory or durophagy (Pritchard 1979; Ernst and Barbour 1989). Adaptations to these ecological specializations have been proposed for different parts of the skeleton. For example, forearm anatomy strongly correlates with aquatic adaptation (Joyce and Gauthier 2004) and shell shape may correlate with habitat ecology (e.g., Claude et al. 2003; Dziomber et al. 2020). Ecomorphological adaptations are also expected in the turtle skull (Claude et al. 2004; Foth et al. 2017), which is their primary tool of interaction with the environment. High neck mobility, including the ability of neck retraction, is an important functional mechanism that enables such interactions, allowing skull movement independent of the rigid shell (Pritchard 1984; Werneburg et al. 2015a,b). This renders turtles as an excellent study case to test the potential influences of ecology and function on skull shape, with broad evolutionary interest.

The ecological evolution of turtles as well as the evolution of neck retraction are only partially understood. Turtle ancestry is a highly debated topic (Rieppel & Reisz 1999; Crawford et al. 2012; Field et al. 2014; Bever et al. 2015; Schoch and Sues 2015). The unshelled species *Eunotosaurus africanus* and *Pappochelys rosinae* were likely terrestrial animals (Lyson et al. 2016; Schoch et al. 2019), although aquatic ecology has been proposed for the partially shelled taxon *Odontochelys semitestacea* (Li et al. 2008; Joyce 2015), suggesting that mixed ecologies may have existed along the turtle stem-lineage. The earliest fully shelled stem-turtles occur in the Late Triassic (Gaffney 1990; Rougier et al. 1995; Joyce 2017) and have more frequently been interpreted as terrestrial based on sedimentological and anatomical evidence, such as forelimb anatomy (Joyce and Gauthier 2004) and shell histology (Scheyer and Sander 2007). Among these, the anatomically best-known taxon *Proganochelys quenstedtii* lacks a fully retractile neck (Gaffney 1975; Werneburg et al. 2015a). Given the inferred neck mobility of representatives of both stem- and crown-lineages (e.g., Gaffney 1975; Werneburg et al. 2015a; Anquetin et al. 2017a), it is possible that neck retraction was present by the origin of the crown-group, having evolved among more crownward stem-turtles. However, such taxa are known mainly from skulls (e.g., Gaffney 1972) or incomplete skeletons (e.g., isolated or articulated cervicals; Matzke et al. 2004; Obraztsova and Danilov 2015) that do not allow direct inference of this trait.

Crown-turtles show two primary modes of neck retraction (i.e., pleurodiran side-ways retraction and cryptodiran vertical retraction), but show secondary losses as well (Pritchard 1979; Werneburg 2015). Given that neck mobility is important for skull use in turtles (Pritchard 1984; Herrel et al. 2008), it seems plausible that the evolution of neck retraction, the ecomorphology of the turtle skull, and the ecological diversification of turtles are related, but this has never been explicitly tested. Fossils provide evidence for an early episode of ecological diversification among crownward stem-turtles. Aquatic habits were present in the ancestor of the turtle crown-group (Joyce and Gauthier 2004; Sterli et al. 2018), evolved from likely terrestrial ancestors by the Mid-Late Jurassic (e.g., *Eileanchelys waldmani*, *Condorchelys antiqua*, paracryptodires; Sterli 2008; Anquetin et al. 2009; Joyce and Lyson 2015). Ecological habitat transitions occurred repeatedly since then. For example, during the marine transitions in extant chelonioid sea turtles, thalassochelydian stem-turtles (Anquetin et al. 2017b; Evers and Benson 2019; Joyce et al. 2021a) and bothremydid and sterogenyine pleurodires (Gaffney et al. 2006; Gaffney et al. 2011; Ferreira et al. 2015), but also during terrestrial adaptation of extant tortoises, box turtles (Testudinidae, *Cuora* geomydids, *Terrapene* emydids; Ernst and Barbour 1989), extinct meiolaniforms (Sterli 2015) and nanhsiungchelyid pantrionychians (Yeh 1966).

Turtles show very diverse skull morphologies, which plausibly reflects adaptation to variation in diets, methods of food acquisition, and other traits (Pritchard 1979; Claude et al. 2004; Ferreira et al. 2015; Foth et al. 2017). Previous geometric morphometric work focused on ecological explanations (e.g., habitat or diet) and on different clade levels, arriving at contrasting ecological signals of skull shape. However, these studies either did not account for phylogenetic structure when testing hypotheses (Claude et al. 2004; Ferreira et al. 2015; Foth et al. 2017), did not include fossils (Claude et al. 2004), or used two-dimensional projections of skulls in different views as a proxy for three-dimensional skull morphology (Ferreira et al. 2015; Foth et al. 2017). Furthermore, the association between turtle skull shape and ecology was never analyzed in a broader context that included additional key functional traits (e.g., neck retraction) distinct from the effects of ecological variables.

We compiled a dataset of three-dimensional skull models of 76 extant and 17 extinct turtles, using computed tomography (CT) scans, comprising representatives of all major clades and encompassing different ecologies (Supporting Information S1). We used three-dimensional geometric morphometrics and phylogenetic comparative statistical tools to evaluate the independent effects of various ecological and functional factors on turtle skull shape, including skull size (i.e., allometry), diet, feeding strategy, habitat, and neck retraction capacity, assessing their correlation with evolutionary changes in the skull shape. We then use these results to infer ecological and functional traits of extinct turtles in a quantitative framework, testing previous hypotheses regarding their ecology.

Material and Methods

MORPHOMETRIC DATASET

We used three-dimensional models of 76 extant and 17 extinct turtle skulls (Supporting Information S1 contains a list

specimens and information on data availability), generated from CT scan images, which we manually segmented with the software Avizo 9.0.0 (Visualization Sciences Group) and Mimics Research 21.0 (Materialise NV, Leuven, Belgium). This sample includes representatives of all major lineages of living turtles, as well as fossil taxa of both crown- (e.g., extinct chelonioids and pelomedusoids) and putative stem-turtles (e.g., the paracryptodire *Eubaena cephalica*, the xinjiangchelyid *Annemys* sp.). Also, it includes species from groups that independently evolved marine habits (e.g., thalassochelydians, bothremydids, protostegids). Fossils were selected based on their relative completeness and low level of deformation and distortion to avoid the influence of taphonomic artifacts (e.g., Kammerer et al. 2020).

We quantified skull shape variation with a new landmarking scheme. This includes 75 single-point type I and II landmarks (Bookstein 1991) for homologous structures, such as the intersections of cranial sutures, and 21 series of sliding semilandmark curves (Gunz and Mitteroecker 2013) for capturing curved margins such as skull emarginations, skull openings (e.g., orbits), or the outer surface of the otic capsule along which the jaw adductor muscles of turtles extend. The triturating surfaces and mandibular condyle surfaces are of ecological interest in turtles, because they are directly related to jaw movements linked to feeding (Pritchard 1979). Due to the complexity of these surfaces, which are often characterized by inconsistently present ridges, we used surface semilandmarks as a third type of landmark, following the procedures described by Schlager (2017; see also Gunz and Mitteroecker 2013; Bardua et al. 2019). Detailed descriptions of all landmarks are found in Supporting Information S2.

We placed the full set of landmarks on a sample of 71 extant turtles ("full landmark dataset" hereafter; Hermanson 2021). As many of our sampled fossils and some of our extant specimens are incomplete, not allowing the placement of all landmarks, we also developed a reduced landmarking dataset that could be applied to a larger sample of 76 extant turtles, as well as to the 17 extinct taxa ("combined partial landmark dataset" hereafter; Hermanson 2021). This second set of landmarks captures the overall skull shape (particularly length, width, and height dimensions of the skull), as well as the shape and position of orbits, mandibular condyles, and triturating surfaces, all of which have been previously described as potential correlates to turtle feeding ecomorphology (e.g., Pritchard 1984; Herrel et al. 2002; Lemell et al. 2002). We further distinguish between two versions of the "partial landmark dataset": one that includes only extant turtles, and another that combines extant and extinct turtles. Both extant-only datasets ("full landmark," "extant partial landmark dataset") were used for hypothesis testing, for which the ecology of specimens is known.

ECOLOGICAL AND FUNCTIONAL VARIABLES

Skull morphology in vertebrates has hypothesized relationships to allometric, ecological, and functional factors. We aimed to quantify the independent effects of these factors by constructing multivariate linear models that then could be used to infer the ecological and functional traits of extinct species, based on skull shape. Throughout this work, we used $\log_{10}$-transformed skull centroid size from our landmarks as a skull size index. This was used to evaluate allometric effects on skull shape (Table 1), and also as a response variable to evaluate influences of other variables on skull size.

We also defined a set of variables to capture variation in diet, feeding strategy, habitat, and neck retraction capacity (Table 1; Supporting Information S1). Each of our explanatory variables are independent, binary categorical variables (i.e., "absent" vs. "present"). These allow to assess if a specific presence of a trait has an effect on skull shape (or size), and differs from approaches taken in many previous studies that use single, multicategory variables (e.g. "terrestrial herbivore" vs "aquatic herbivore" for turtles in Foth et al. [2017]; forelimb webbing-based gradient of aquaticness for turtles in Foth et al. [2019]; dietary gradients including herbivory and different types of carnivory for musteloid mammals in Law et al. [2018]; habitat gradient for crocodylomorphs in Godoy [2020]), which are harder to interpret.

Diet was coded using binary variables that describe the presence or absence of 13 specific food items (e.g., "worms," "fruits," etc.), which were then summarized to two dietary preferences "faunivory" and "herbivory."

We also used the 13 food items to derive two continuous traits, namely, a "hardness" and an "evasiveness" index (as in Vanhooydonck et al. 2007), which describe physical or behavioral properties of main food items proportionally present in turtle diets (see Supporting Information S2 for further details).

We recorded two variables ("durophagy," "suction feeding") regarding specific feeding modes of some turtles. These are binary variables to test if these feeding strategies indeed have a strong effect on skull shape, as commonly suggested (e.g., Pritchard 1984; Joyce et al. 2021b). The use of "suction feeding" in the turtle literature is somewhat ambiguous, and sometimes used for all aquatic feeders (due to compensatory suction employed during forward head movements; Van Damme and Aerts 1997), or limited to chelids (Lemell et al. 2002). Here, we mostly classify aquatic turtles that hunt active prey as suction-feeders (e.g., trionychids and chelids; see Supporting Information S1 and S2 for full details), but also include species for which there is empirical data on the use of this feeding strategy (e.g., *Dermochelys coriacea*; Bels et al. 1998).

Feeding habitat was coded using presence/absence for traits describing where turtles feed ("in the water" and/or "on land"), whereby these are not exclusive and encode the capacity of a

Table 1. Variables used for building multiple phylogenetic regressions. The biological question behind each variable changes to "are there independent effects of these variables" in complex models. Skull size is used as an explanatory variable in shape regressions, but as the response variable in size regressions. Carapace length as a body size index is used as an allometric explanatory variable in size regressions.

Variable	Variable type	Biological question
Log_{10}(skull centroid size)	Allometric	Is there an effect of skull size on skull shape?
Log_{10}(maximum straight carapace length)	Allometric	Is there an effect of body size on skull size?
Log_{10}(neck length)	Morphofunctional	Is there an effect of neck length on skull shape/size?
Neck retraction	Morphofunctional	Is there an effect of neck retraction on skull shape/size?
Faunivory	Dietary	Is there an effect of faunivory on skull shape/size?
Herbivory	Dietary	Is there an effect of herbivory on skull shape/size?
Durophagy	Feeding mode	Is there an effect of durophagy on skull shape/size?
Suction feeding	Feeding mode	Is there an effect of suction feeding on skull shape/size?
Food evasiveness	Food properties	Is there an effect of food evasiveness on skull shape/size?
Food hardness	Food properties	Is there an effect of food hardness on skull shape/size?
Terrestrial feeding	Feeding habitat	Is there an effect of terrestrial feeding habits on skull shape/size?
Aquatic feeding	Feeding habitat	Is there an effect of aquatic feeding habits on skull shape/size?
Marine	Marine habitat	Is there an effect of marine habitat on skull shape/size?
Flippered	Locomotion type	Is there an effect of specialized aquatic locomotion on shape/skull size?

species to feed on land (or in water) without regard to the frequency of that behavior. Turtles that show foraging behavior both on land and in water are thus scored as "present" for both habitat traits. We also encoded whether a species is marine or not. All of these habitat traits have been previously suggested to correlate with shape changes in the turtle skull (e.g., Bramble and Wake 1985; Hirayama 1998; Natchev et al. 2015; Lemell et al. 2019).

We also encoded whether forelimbs are flippered or not (as a proxy for an open-swimming, fully aquatic lifestyle, as present in chelonioid sea turtles and *Carettochelys* today).

Because previous studies suggested a relation between skull shape and neck movements (Werneburg 2015; Ferreira et al. 2020), we considered a binary functional variable scoring the capability of turtles to withdraw their necks (i.e., neck retraction). Finally, we also considered neck length/carapace length ratio as an explanatory variable, since the evolution of longer necks has been proposed to correlate with specialized predatory lifestyles (e.g., Van Damme and Aerts 1997; but see Alcaldade et al. 2010). For this test, we used the "Carapace neck ratio [%]" data from Joyce et al. (2021b). We expanded their dataset and pruned the data to our sample of extant species, totaling 60 species with neck/carapace ratio information within the "full landmark dataset" and 65 within the "partial landmark dataset." When multiple specimens per species were available, we used the mean of their values (see Table S1 for relative neck length data). The analyses with these smaller datasets are included in Supporting Information S2.

GEOMETRIC MORPHOMETRIC ANALYSES

We performed Generalised Procrustes Analysis (GPA; Gower 1975) to remove the effects of size, position, and orientation of the skull from the original landmarks across different datasets. Sliding semilandmarks were moved along their tangent vectors to minimize bending energy differences from the mean shape (Webster and Sheets 2010; Gunz and Mitteroecker 2013). All geometric morphometric and statistical analyses were conducted in R 4.0.2 (R Core Team 2020). R scripts are provided in Hermanson (2021). GPA was performed using the "gpagen" function from the "geomorph" 3.2.1 package (Adams et al. 2020). The surface semilandmarks were placed on a template specimen (i.e., the specimen with the closest shape to the estimated mean for a set of aligned coordinates) and then projected to the other specimens in an automated process. This step was performed using the "placePatch" function from the "Morpho" 2.8 package

(Schlager 2017). Then we ran a GPA on all landmarks combined (point landmarks, semilandmark curves, surface semilandmarks). This entire procedure was repeated three times, for each of our datasets ("full landmark," "extant partial landmark," "combined partial landmark").

Procrustes coordinates were used to conduct a Principal Component Analysis (PCA) to visualize the principal component axes (PCs) of variation in turtle cranial shape for the "full landmark" ($N = 71$) and "combined partial landmark" ($N = 93$) datasets. We could therefore assess how turtle cranial morphospace changes with the inclusion of extinct taxa. This was performed using the "plotTangentSpace" function from "geomorph" 3.2.1 (Adams et al. 2020).

The three-dimensional Procrustes coordinates of the extant-only datasets were used as shape data for hypothesis tests, whereas the $\log_{10}$-transformed skull centroid size was used as a proxy for skull size in downstream analyses.

ECOMORPHOLOGICAL HYPOTHESES—SKULL SHAPE

We evaluated the relationships between skull shape and our ecological and functional traits using phylogenetic Procrustes distance-based multivariate regressions (D-PGLS; Adams 2014; Adams and Collyer 2018a), using the "procD.pgls" function of "geomorph" 3.2.1 (Adams et al. 2020). These analyses included only the extant species sampled in both our "full landmark" ($N = 71$ extant species) and "partial landmark" ($N = 76$ extant species) datasets. For the phylogenetic framework, we used the time-calibrated molecular phylogeny of Pereira et al. (2017) pruned to our taxon sample (Fig. S6).

Our allometric, ecological, and functional variables individually represent questions such as "What is the effect of skull size on skull shape?" and "Is there an effect of marine adaptation on skull shape?" (Table 1). Therefore, our core hypotheses occur at the level of individual explanatory variables, of which we included 13 in total (Table 1). However, these variables show possible interdependencies. For example, marine turtles show large sizes on average compared to terrestrial turtles. This requires statistical models including multiple explanatory variables to quantify the independent effects of our variables. We therefore aimed to find the combination of explanatory variables that had the greatest explanatory power, without overfitting. Typically, this would be achieved using information criteria such as Akaike information criterion (AICc). We were able to use this for phylogenetic generalized least squares regressions of skull size (pGLS, described below). However, such methods have not yet been developed for analysis of multivariate dependent variables and so could not be applied to our D-PGLS analyses of skull shape (Adams and Collyer 2018b; Clavel et al. 2019). We therefore approached model comparison as follows (and for similar approaches, see Bronzati et al. 2021; Lowi-Merri et al. 2021; Marek et al. 2021; Evers et al. unpubl. ms.):

Preliminary analysis showed that skull centroid size had a strongly significant relationship to skull shape, regardless of other variables. We therefore included this in all models. We then evaluated the potential importance of other variables by including them individually alongside skull centroid size in a series of simple models (i.e., skull shape ~ skull size + variable) reported in Tables S4 and S5. We then constructed a model including all variables that were returned as significant in the initial round of analyses. This rendered some variables as nonsignificant, which were then removed. Our best model is thus that with the highest coefficient of determination (R^2) in which all variables have significant and independent effects.

We evaluated a somewhat large number of hypotheses simultaneously, evaluating 13 variables in total, with potential to introduce false positives through carrying out multiple comparisons. Our model is primarily used to infer the ecological and functional traits of extinct species. Therefore, we view controlling for the independent effects of confounding variables as being important, confirming the necessity to evaluate as many of the potential influences on skull shape as possible. We addressed potential problems with overfitting by using the "false discovery rate (FDR)" method (Benjamin and Hochberg 1995) for P-value correction. Besides reducing false positives, this method also minimizes the rate of false negatives (Jafari and Ansari-Pour 2019).

To test the hypothesis that anteroventral and posterodorsal skull emarginations correlate with one another, as proposed by Werneburg (2015), we also carried out a phylogenetic two-block partial least squares analysis (2B-PLS; Rohlf and Corti 2000; Adams and Felice 2014), using the respective semilandmark series from the "full landmark dataset." 2B-PLS assesses the structure of covariance between two shape blocks. This analysis was performed using the "phylo.integration" function of "geomorph" 3.2.1 (Adams et al. 2020).

ECOMORPHOLOGICAL HYPOTHESES—SKULL SIZE

We evaluated the relationships between skull size and our ecological and functional traits using phylogenetic generalized least squares regressions (pGLS; Grafen 1989), implemented using the function "gls" in the R package "nlme" 3.1-148 (Pinheiro et al. 2020), and correlation structures from "ape" 5.0 (Paradis and Schliep 2019), for $N = 71$ extant species. We used all of the variables listed in Table 1, additionally including $\log_{10}$-transformed carapace lengths from TTWG (Rhodin et al. 2021) as a body size index, to account for allometric effects. These maximum, adult straight carapace lengths were compiled from the literature and not directly derived from the specimens used to quantify skull shape. However, we do not think this is a problem, because (a) the skulls used are predominantly from large adult individuals,

and (b) because ontogenetic shape differences among species are small in turtles in comparison to interspecific shape variation (e.g., Nishizawa et al. 2010; Foth et al. 2017). We built pGLS models by combining multiple sets of independent variables. Instead of the iterative procedure used for shape regressions, we compared a slightly larger number of models ($N = 20$) using AICs for finite samples (Sugiura 1978; Burnham and Anderson 2002). For this, we used the "aictab" function from the package "AICcmodavg" 2.3-1 (Mazerolle 2020). We estimated phylogenetic signal of model residuals (λ; Pagel 1999) during the model-fitting process. The R^2 for these models was calculated using the "R2" function from the "rr2" 1.0.2 package (Ives 2019).

EXAMINATION OF SHAPE CHANGE IN RESPONSE TO ECOLOGICAL AND FUNCTIONAL TRAITS

We used R "stats" routine functions (R Core Team 2020) to visualize the independent effects of specific predictors on turtle skull shape. We implemented this by varying the score of each predictor individually, while holding the scores of all the other variables constant at their most frequent value among sampled species (for presence/absence variables) or at their mean value (for continuous traits such as $\log_{10}$-skull size). We used first and third quartiles of continuous traits instead of minimum and maximum values to avoid outliers. We then normalized the Euclidean distance between the points of the two sets of resulting shapes to graphically inspect the variation from one condition to the other. Alternatively, we also visualized the variation between minimum and maximum values of such sets of points with heat maps using the "procrustes.var.plot" function of the "landvR" 0.5.2 package (Guillerme et al. 2021). These include vectors that indicate the directional changes of each specific landmark, and are available in Supporting Information S2.

In practice, the shape variation associated with each predictor can be extracted from the vector of coefficients of that predictor in the D-PGLS model (or "coefficient vector"). This vector represents the shape axis in multivariate space that best distinguishes between different values of our predictor variables, after (i) excluding the effects of phylogenetic effects that would otherwise introduce "false positive" elements of covariance between skull shape and predictor variables (e.g., Felsenstein 1985); and (ii) excluding the effects of other predictor variables from the regression model to resolve the independent effect of each variable on its own (e.g., independent of allometry and the effects of other ecological traits).

We also retrieved regression scores (as defined in Drake and Klingenberg 2008) for each specimen on each predictor from the best D-PGLS models (i.e., with the greatest R^2 value). These regression scores result from the projection of the multivariate shape data of turtle skulls onto the coefficient vector for each predictor in the D-PGLS model. The regression score of a specimen therefore represents the extent to which that specimen resembles the predicted shape for a value of a predictor variable. Because our approach makes use of the independent effect each variable has in a multiple regression mode, we could assess the relationship between different shape predictors individually, and also represent these in a multivariate ordination morphospace to graphically visualize whether the presence of a particular trait might constrain the presence of another. To calculate these, we used a customized R code (Hermanson 2021).

PREDICTIONS FOR FOSSILS

As fossils were not included in the D-PGLS models, their regression scores for each predictor variable could not be directly extracted from the D-PGLS outputs. Therefore, we separately projected the skull shapes of fossil turtles onto the coefficient vectors of the D-PGLS based on the "partial landmark dataset" using custom code (Hermanson 2021). This allowed us to visualize the extent to which fossil specimens resembled the expected shapes for each of our predictor variables. We also used these regression scores as input to infer the ecological traits of fossil species.

We used phylogenetic flexible discriminant analysis (pFDA) to formally evaluate the posterior probability (PP_{trait}) that fossil taxa exhibited specific ecological or functional variables (i.e., those traits found to have a significant relationship with skull shape in our D-PGLS analyses). We conducted pFDA using the regression scores instead of the full shape data (i.e., Procrustes coordinates) because our D-PGLS analyses indicate the importance of multiple predictor variables, some of which are partially co-linear with one another. This would introduce confounding effects to a pFDA based on shape data if no attempt was made to identify the independent effects of specific predictors separate from one another (e.g., removing the effects of allometry and confounding ecological traits). pFDA was implemented using custom R functions from Motani and Schmitz (2011). Following Chapelle et al. (2020), we trained our discriminant function by iteratively resampling our dataset, running 100 replicates of pFDA. Success rates were calculated as the proportion of correct interpretations of ecology for extant species from shape data alone. In the end, we extracted the mean PP_{trait} of fossil turtles and considered a value of ≥ 0.66 to represent "likely presence," $0.33 \geq PP_{trait}$ as "likely absence," and $0.33 < PP_{trait} < 0.66$ as "uncertain" for a given trait. Posterior probabilities should be evaluated in combination with success rates for the correct classification of ecological variables for extant turtles. For example, in a high success rate of 95%, accepting a PP of >0.66 is quite conservative.

For the pFDA, we used two time-calibrated phylogenetic trees that represent alternative topologies (Evers et al. 2019 [strict consensus]; Sterli et al. 2018 [MkA model]). They differ in the placement of some fossil clades with respect to extant turtles, the relationships of which follow a molecular consensus (Pereira

et al. 2017). We chose these alternative topologies to account for the phylogenetic uncertainty on the position of secondarily marine turtles from the Jurassic-Paleocene. Both trees are fully disclosed in Supporting Information S2 (Fig. S7). Nevertheless, because the PP_{trait} calculated for the fossils was nearly identical on both topologies (Table S11), we present only the results based on the topology of Evers et al. (2019).

We predicted the "evasiveness index" for fossils, because this was the only continuous ecological trait present in the best D-PGLS model using the "partial landmark dataset" (Table S8). We first ran pGLS analyses to assess which combination of regression scores from the D-PGLS model best explained such index for extant turtles, using the "phylostep" function from the R package "phylolm" 2.6.2 (Ho and Ané 2014). We then obtained these values using the "predict" function from R "stats" (R Core Team 2020). To visualize the distribution of all of these traits predictive of skull shape among turtles, we mapped them onto the Evers et al. (2019) topology using graphical tools from the R package "phytools" 0.7-70 (Revell 2012).

Results

Our principal component analyses (PCAs) describe major aspects of turtle skull variation, among extant (Fig. 1a,b) and extant plus fossil taxa (Figs. 1c,d, S3–S5). The first two axes of our PCA with the "full landmark dataset" contain nearly 50% of shape variation and overall depict changes in aspects such as general proportions (e.g., skull height and length), extent of emarginations, and shape of the triturating surfaces of the palate. PC1 accounts for 28.2% of shape variation, with positive values describing skulls with a high braincase and anteroventrally sloping skull roof, short supraoccipital crests, a weakly pronounced otic trochlear process, a reduced posterodorsal emargination, and a more extensive anterolateral emargination, as seen in chelonioids, chelids, and some pelomedusoids. Negative PC1 values describe skulls with relatively longer supraoccipital crests, reduced anterolateral emargination, more extensive posterodorsal emargination, in addition to an acutely angled preorbital snout region, as seen in trionychians and some chelydroids (Fig. 1a). Positive values of PC2 (20.6%) describe dorsoventrally flattened skulls, with dorsally oriented eyes, greater anterolateral emargination, posteriorly elongated squamosals, and flat palates, including narrow triturating surfaces (e.g., long-necked chelids and trionychids; Fig. 1b). Negative PC2 values describe taxa possessing high-domed skulls, laterally placed orbits, a short ventral exposure of the basisphenoid, less developed anterolateral emarginations, a broad area for the triturating surfaces, and a more vaulted palate (e.g., the pelomedusoid *Peltocephalus dumerilianus*, chelonioids, and testudinids). Overall, the first two PC axes show a strong trade-off regarding the extent of both skull emarginations (Fig. 1b). This is further supported by our 2B-PLS analysis (r-PLS = 0.756; P = 0.001; effect-size = 6.37), which shows that, in general, when one emargination is large, the other is reduced (Fig. 2b). Exceptions to this occur in turtles with reduced emarginations, such as sea turtles, *Peltocephalus*, and *Platysternon*, for instance.

In the PCA using the "partial landmark dataset," extant taxa are structured differently both in terms of the distribution of the clades and the morphological features described along the PC axes (Fig. 1c,d). Positive values of PC1 (25.2%) describe anteroposteriorly long and dorsoventrally low skulls, with dorsally oriented orbits and posteriorly displaced mandibular condyles (Fig. 1d), such as those of some chelids and trionychians. Negative PC1 values describe cranial shapes with increased height and reduced length, in addition to more lateralized orbits (Fig. 1d), such as those of sea turtles and tortoises. The second axis (PC2; 19%) describes changes in the width of the preorbital area, as well as in the palate shape. Positive PC2 values include skulls with a narrow preorbital area, with pointed beaks and mediolaterally expanded triturating surfaces (e.g., most chelonioids, some geoemydids; Fig. 1c,d), whereas negative PC2 values describe skulls with a wide preorbital area, rounded beaks, and extremely narrow triturating surfaces (Fig. 1d), as seen in both extinct (e.g., *Sahonachelys mailakavava*) and extant taxa (e.g., *Chelus fimbriatus*).

The changed relative importance of specific skull aspects on the principal component axes in the analysis using the "partial landmark dataset" (see Fig. 1c,d vs. 1a,b) is primarily caused by the different landmark dataset itself: When fossils are excluded from the "partial landmark dataset" (Fig. S4), the relative distribution of extant datapoints remains the same as when fossil are included (Figs. 1c,d, S5). However, similar associations of landmarks control the extremes along PC axes across both datasets. For instance, differences between flat and long skulls (e.g., trionychids) versus high and short skulls (e.g., chelonioids) determine PC2 when the "full landmark dataset" is used, but gain relative importance using the "partial landmark dataset," in which they determine shape variation along the first axis (PC1). The inclusion of fossils in our second PCA then simply expands the limits of the extant morphospace (Fig. S5), but have little additional effect on the primary controls on the PC axes. For both extant clades for which we could include fossil specimens (i.e., chelonioids and pelomedusoids), disparity is notably expanded in terms of occupied morphospace area, indicating that fossils of these groups document skull shape diversity that is not found in their modern representatives. For pelomedusoids, fossil taxa even protrude into regions of the morphospace not occupied by extant species, documenting skull shapes not found among any modern species, such as *Ummulisani rutgersensis* with its high-domed skull, dorsolateral eyes, and preorbital boss (Gaffney et al. 2006).

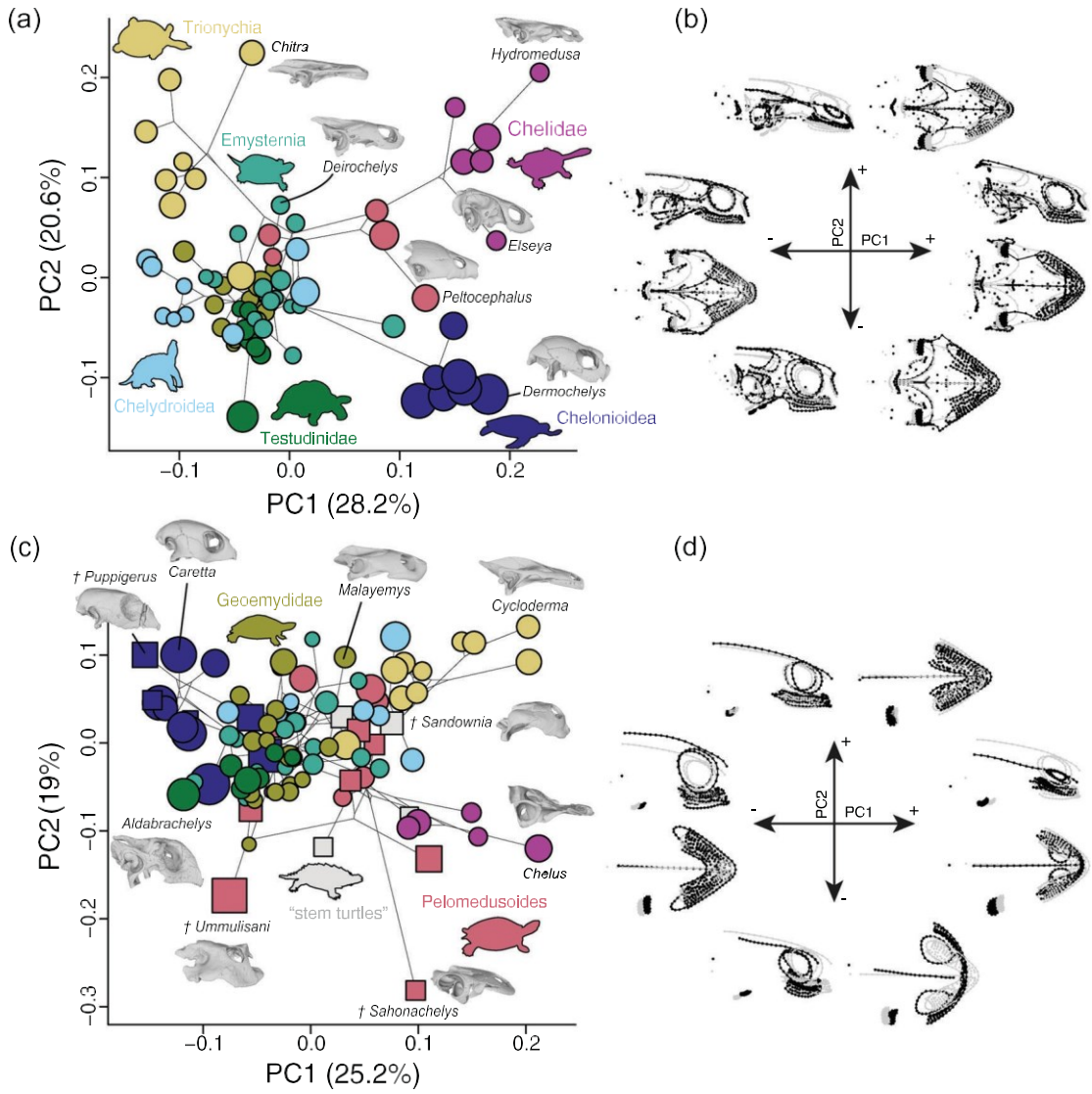

Figure 1. **Skull shape variation among turtles. (a) PC1 and PC2 axes of shape variation among extant turtles only (*N* = 71), projected onto the topology of Pereira et al. (2017). (b) Landmark configurations corresponding to PC1 and PC2 extreme values (black) superimposed onto the mean shape (gray). (c) First (PC1) and second (PC2) axes of shape variation among extant and fossil turtles (*N* = 93), projected onto a composite topology based on Evers et al. (2019). (d) Landmark configurations corresponding to PC1 and PC2 extreme values (black) superimposed to the mean shape (gray). Point symbol sizes correspond to skull size variation among the sampled specimens, scaled to the turtle with the largest skull centroid value (Dermochelys). Circles indicate extant taxa, whereas squares denote fossils. See Figure S3 for individually labeled taxa.**

The AICc-best performing pGLS model to explain skull size variation in turtles, in which all variables were statistically significant, includes a combination of overall size effects (carapace size) and the ability for neck retraction (Table 1; "skull size ~ carapace size + neck retraction"). Carapace size was statistically significant in all models (Table S2), and its coefficient (0.57 in the best model, compared to 1.0 under isometry; Table S2) indicates strong negative allometry of skull size in relation to body size (Fig. 2a). The coefficient of neck retraction ($slope_{neck\_retraction} = -0.21$; $SE_{coef} = 0.04$; $P < 0.001$) indicates that turtles that can fully retract their necks have relatively smaller skulls than those incapable of it, and this effect was also significant across all models with nonnegligible AICc weights. Other nonnegligible models additionally include ecological variables, specifically "durophagous" (no | yes), "open swimming" (no | yes), "marine" (no | yes), and "food hardness index". Two of these ("open swimming" and "marine") are significant on their own in bivariate models, indicating that their nonsignificance in multivariate models can be explained by their effects being redundant with that of neck retraction. These results show that

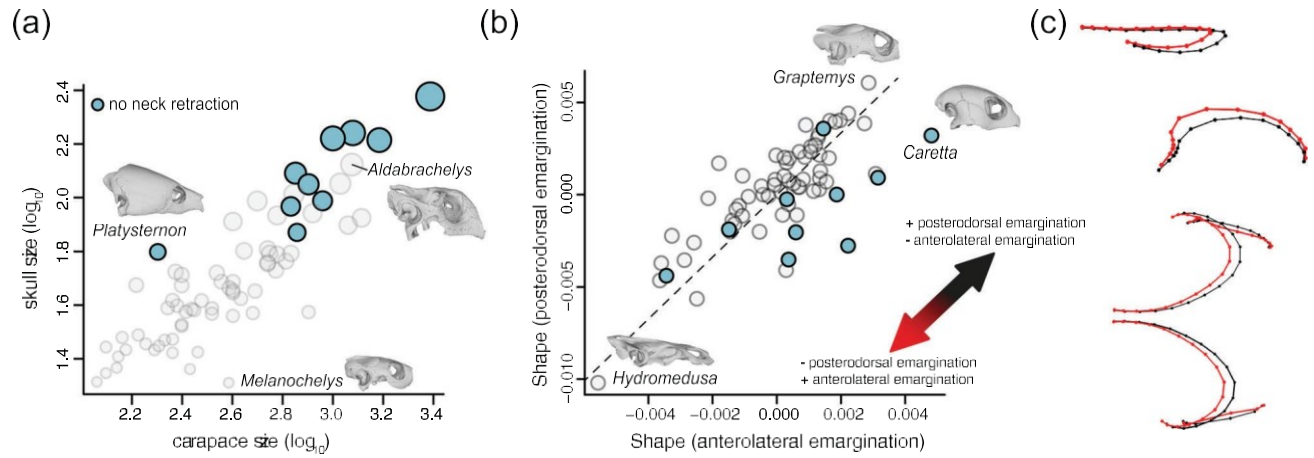

Figure 2. Size relationships and emargination aspects of turtle skulls. (a) pGLS regression ($N = 71$) of skull size on carapace size of extant turtles, with taxa unable of neck retraction highlighted. Three-dimensional models of *Platysternon megacephalum* and *Melanochelys trijuga* indicate turtles with the largest and smallest heads relative to their body size. Point size corresponds to relative skull size, scaled to the turtle with the largest skull centroid value (*Dermochelys coriacea*). (b) Phylogenetic 2B-PLS ($N = 71$) between shape of turtle skull emarginations, indicating an inverse pattern in their extent. Three-dimensional models of *Graptemys geographica*, *Caretta caretta*, and *Hydromedusa tectifera* indicate extreme values. (c) Landmark configurations of the minimum (red) and maximum (black) of each axis in right lateral (top) and dorsal (bottom) views. See Figure S23 for individually labeled taxa.

ecology has no significant effect on skull size in turtles. Analyses of the smaller dataset ($N = 60$) including neck/carapace ratio as an explanatory variable indicate no significant relationship between relative neck length and skull size in any model (Table S3).

For skull shape, our models recovered significant independent effects of size-related, functional, and ecological variables. The D-PGLS best model using the "full landmark dataset" takes the form of "skull shape ~ skull size + neck retraction + aquatic feeding + suction + durophagous + hardness + evasiveness." The best model using the "extant partial landmark dataset" is only slightly different: "skull shape ~ skull size + neck retraction + suction + durophagous + evasiveness" (Table 2), indicating that the differences in our two landmark datasets have no strong effect on our ecomorphological analyses and interpretations. All variables individually explain only small proportions of skull variation (2%−4.9%), and all significant variables together only explain 18.4%−21.8% of the skull variation (Tables 2, S4, and S5). Analyses of the smaller "full landmark dataset" ($N = 60$), which includes relative neck length as a variable, indicate a potential relationship between this trait and skull shape, with relatively longer necks corresponding to more elongate skulls with larger posterodorsal emarginations (Table S6). This agrees with previous proposed associations between increasingly longer necks and deeper emarginations throughout turtle evolution (Dalrymple 1979; Ferreira et al. 2020). However, when using the smaller "partial landmark dataset" ($N = 65$), the effect of relative neck length is nonsignificant if included together with the evasiveness index as an explanatory variable (Table S7), and the best model remains the same as that with greater sample size (i.e., $N = 76$; see above). This suggests relative neck length to have importance in the feeding ecology of turtles, as turtles that specialize on more elusive prey tend to have relatively longer necks (e.g., Van Damme and Aerts 1997; Joyce et al. 2021b).

Skull size (representing evolutionary shape allometry) is consistently found to be significant across all D-PGLS models and consistently has large effect sizes (see *Z*-values in Table 3; Tables S4 and S5). Its coefficients indicate that taxa with relatively larger skulls have anteroposteriorly shorter skulls, with prominent anterior displacement of certain skull features such as the occipital condyle and the foramen magnum (Figs. 3a, S8, S9). Our functional variable "neck retraction" (i.e., the presence thereof) correlates with low, anteroposteriorly lengthened skulls with prominent emarginations. Turtles that do not retract their necks possess dorsoventrally high and anteroposteriorly short skulls, in which the posterior region is markedly short, and both emarginations are extremely reduced (Fig. 3a).

Our significant ecological variables show that feeding in an aquatic environment has effects on skull shape among turtles, and that this shape is further modified in aquatic feeders that follow different feeding strategies (Figs. 3a, S8–S15). Aquatic feeding correlates with flattened skulls, narrow palates and external nares, and posteriorly elongate supraoccipital and squamosal processes (Fig. 3a). This variable, however, was only significant when at least "skull size" was also included in the same model (Table S4), indicating aquatic feeding explains turtle skull shape only when allometric effects are considered. Aquatic feeding strategies affect aspects of skull shape intuitively linked to feeding, particularly aspect ratios, shape and position of orbits, shape of

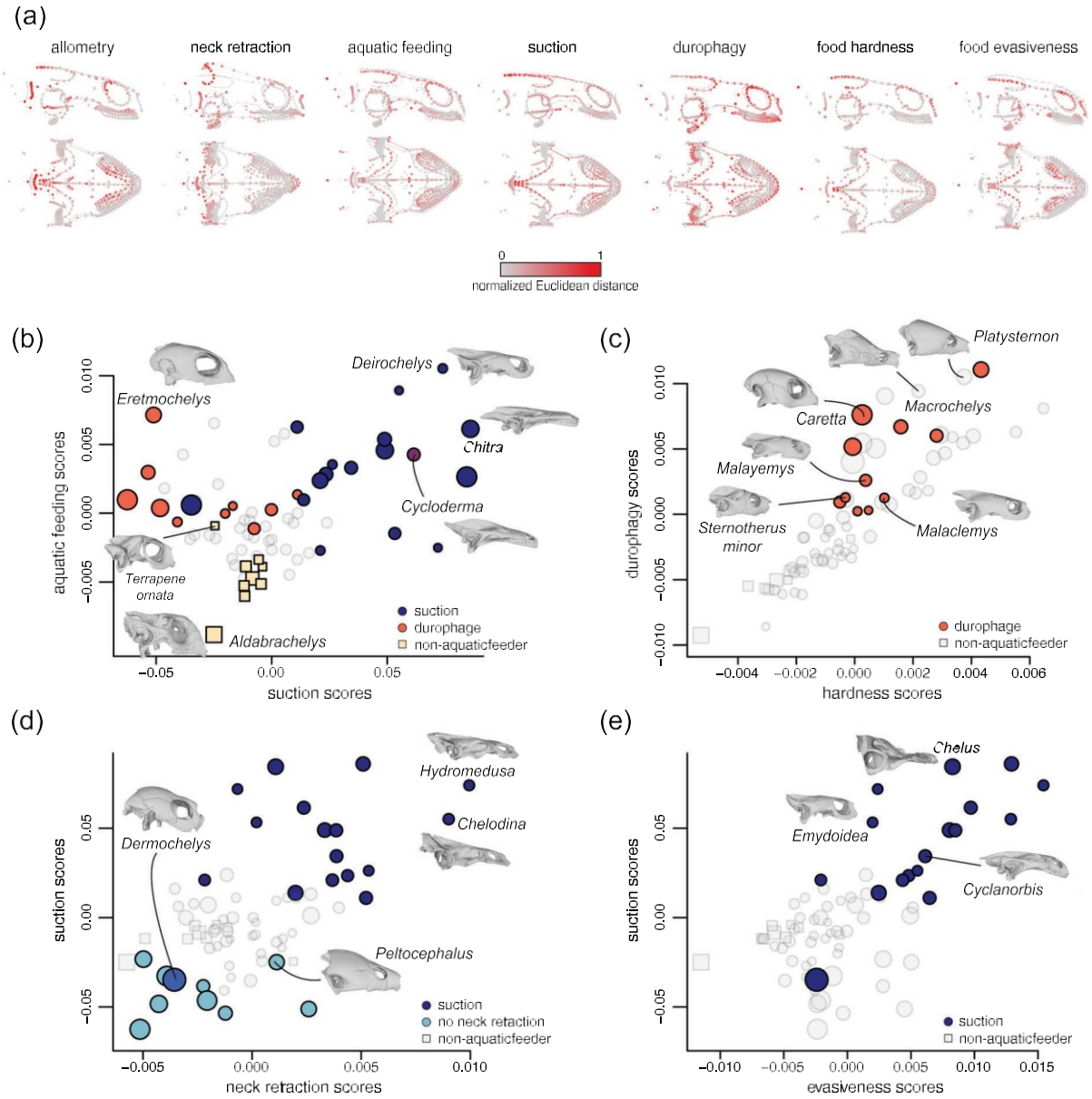

Figure 3. Relationships of skull shape and predicted versus observed ecology in turtles. (a) Predicted shape changes associated with individual ecological variables. Variable-specific landmark deformations (red-scale) with regard to shape configuration excluding the effect (gray), shown in right lateral and ventral views, were extracted from best D-PGLS model using the "full landmark dataset" ($N = 71$). See Figure S9-S15 for alternative plots with vectors indicating the direction of change for each landmark. (b-e) Multivariate morphospaces of the regression scores for selected variables taken from the best D-PGLS models using the "full landmark dataset." High scores indicate a close resemblance of the skull shape of a species with the predicted skull shape for the respective ecological variable. True (i.e., observed) ecological attributes are denoted with color in the respective plots, and allows for a visual appreciation of prediction accuracy. For instance, note high correspondence of suction score values (prediction) with suction-feeding habits (dark blue) across plots, but high number of uncolored data points along positive values for the durophagy axis in (c), indicating that some turtles without durophagous habits have skull shapes corresponding to durophagous D-PGLS predictions. *Cycloderma frenatum* was colored differently in panel (b) to indicate presence for both "suction" and "durophagy" traits, whereas *Dermochelys coriacea* was colored differently in panel (d) to jointly indicate presence for "suction" and absence for "neck retraction." Point size corresponds to relative skull size, scaled to the turtle with the largest skull centroid value (Dermochelys). See Figure S24 for individually labeled taxa.

Table 2. Phylogenetic regressions (pGLS) of turtle skull size (centroid size from the "full landmark dataset," $N = 71$) using size-related, ecological, and functional traits as explanatory variables. AICc-best model on top.

Model	λ	R^2	AICc	AICc weight	Variable	Coefficient	*P*-value
Skull size ~ carapace size + neck retraction	0.13	0.806	−103.31	0.35	(Intercept)	0.41	**0.010**
					Carapace size	0.57	**<0.001**
					Neck retraction	–0.21	**<0.001**
Skull size ~ carapace size + open swimming + neck retraction	0.14	0.810	–101.91	0.17	(Intercept)	0.42	**0.020**
					Carapace size	0.56	**<0.001**
					Open swimming	0.07	0.330
					Neck retraction	–0.17	**<0.01**
Skull size ~ carapace size + marine + open swimming + neck retraction	0.10	0.813	–101.30	0.13	(Intercept)	0.43	**0.020**
					Carapace size	0.56	**<0.001**
					Marine	–0.18	0.180
					Open swimming	0.18	0.100
					Neck retraction	–0.21	**0.004**
Skull size ~ carapace size + neck retraction + food hardness	0.15	0.807	–101.02	0.11	(Intercept)	0.43	**0.010**
					Carapace size	0.57	**<0.001**
					Neck retraction	–0.21	**<0.001**
					Food hardness	–0.01	0.730
Skull size ~ carapace size + neck retraction + durophagous	0.13	0.806	–100.93	0.11	(Intercept)	0.40	**0.026**
					Carapace size	0.57	**<0.001**
					Neck retraction	–0.20	**<0.001**
					Durophagous	0.00	0.910
Skull size ~ carapace size + marine + neck retraction	0.13	0.806	–100.91	0.11	(Intercept)	0.41	**0.021**
					Carapace size	0.57	**<0.001**
					Marine	0.00	0.990
					Neck retraction	–0.21	**0.004**

***Note*: Continuous size values were all $\log_{10}$-transformed prior to analyses. Only nonnegligible models shown; full set of results are included in Supporting Information S2. λ, phylogenetic signal (Pagel's lambda) of residuals estimated as part of the model-fitting process; R^2, coefficient of determination of the model; *P*-value, corrected *P*-value using the "FDR" method (see *Material and Methods*). Raw *P*-values are included in Table S2. Numbers in bold denote significance at $\alpha < 0.05$; AICc, scores of AIC for small samples; AICc weight, relative importance of the model. $N = 71$ for analyses.**

the palate, and shape of the temporal and emargination areas, which are spaces housing adductor muscles. Suction-feeding implies lengthening of the overall cranial shape and narrowing of the palate and anteriorly placed orbits. Preying on elusive prey (i.e., higher "evasiveness index") correlates to a noticeable decrease in skull height, enlargement of the abductor chamber area, and more laterally placed mandibular condyles. Main shape deformations related to durophagous habits are mediolaterally broadening of the palate and an increase in the posterodorsal emargination extent. The effects of higher "hardness index" values on skull shape point to an increase in the supraoccipital length, as well as a slight increase in overall skull height and a minor widening of the triturating surfaces. Although all these variables have significant independent effects, the variables "suction" and "durophagy" are partially redundant with "evasiveness" and "hardness," respectively, as indicated by changes in their R^2 values between multiple and bivariate regressions (Table S4).

Our phylogenetic discriminant analyses correctly classify between 77% and 93% of extant turtles based on their regression

Table 3. Best models of phylogenetic Procrustes distance-based regressions (D-PGLS) of turtle skull shape (Procrustes coordinates) for the different morphometric datasets: "Full landmark dataset" (*N* = 71) on top; "Partial extant landmark dataset" (*N* = 76).

Model	*N*	R^2 model	Variable	Effect	*Z*-score	R^2	*P*-value
Shape ~ skull size + neck retraction + aquatic feeding + suction + durophagous + hardness + evasiveness	71	0.217	Skull size	Allometric	3.859	0.045	**0.003**
			Neck Retraction	Functional	4.206	0.048	**0.003**
			Aquatic feeding	Ecological	1.702	0.020	**0.040**
			Suction	Ecological	2.366	0.025	**0.015**
			Durophagous	Ecological	2.910	0.029	**0.005**
			Hardness	Ecological	1.883	0.020	**0.037**
			Evasiveness	Ecological	2.937	0.029	**0.004**
Shape ~ skull size + neck retraction + suction + durophagous + evasiveness	76	0.184	Skull size	Allometric	3.600	0.043	**0.002**
			Neck retraction	Functional	2.966	0.036	**0.005**
			Suction	Ecological	1.830	0.021	**0.033**
			Durophagous	Ecological	3.647	0.044	**0.002**
			Evasiveness	Ecological	3.249	0.041	**0.003**

***Note*: Full set of results are included in Supporting Information S2. R^2, coefficient of determination of each individual predictor; *P*-value, corrected *P*-value using the "FDR" method (see *Material and Methods*). Raw *P*-values are included in Tables S4 and S5. Numbers in bold denote significance at $\alpha < 0.05$; R^2 model, sum of R^2s of individual predictors in the model.**

scores, depending on which trait was predicted (Tables S9 and S10). Suction-feeding and durophagy had high correct classification rates (93% and 88%), whereas neck retraction was only correctly classified in 77% of species. Misclassifications for neck retraction exclusively were turtles that retract their necks, but which were predicted not to do so (e.g., the Aldabra giant tortoise *Aldabrachelys gigantea*). Feeding misclassifications are concentrated in clades with high feeding disparity, but similar skull shape (possibly indicating phylogenetic constraints), such as chelonioids. For instance, *Dermochelys coriacea* was predicted as not being a suction-feeder, or *Natator depressus* was predicted to be durophagous. The skulls of misclassified turtles showed variable deviations from the inferred shape for a given predictor (e.g., high in *D. coriacea*; low in *N. depressus*; Figs. 4a, S17–22).

Neck retraction is predicted as uncertain in the baenid stem-turtle *Eubaena cephalica* (PP = 0.58), but other stem-turtles included in our analysis, including xinjiangchelyids and thalassochelydians, are predicted as being capable of neck retraction with high posterior probabilities (PP = 0.9−1). Given that classification failures in the training set (23% classification failures, compared to 77% posterior predictive success) almost exclusively result from misclassification of turtles that have neck retraction as lacking it, we have high confidence in the predictions for presence of neck retraction in extinct species analyzed here. Low and intermediate posterior probabilities (indicating absence of neck retraction, or uncertainty) were limited to crown-group turtles with high-domed skulls and previously proposed marine habits, including pleurodires (*Phosphatochelys tedfordi*, *Bairdemys hartsteini*, *Galianemys emringeri*, and *Ummulisani rutgersensis*) and extinct chelonioids (e.g., *Eochelone brabantica*, *Argillochelys antiqua*, and *Rhinochelys pulchriceps*).

Suction-feeding, for which we had high prediction accuracy in our training dataset, was predicted for the xinjiangchelyid *Annemys* sp., the thalassochelydian *Sandownia harrisi*, and three taxa representing different pleurodire lineages (*Sahonachelys mailakavava*, *Labrostochelys galkini*, and *Lapparentemys vilavilensis*). Our results for durophagy prediction in fossils include (1) instances in which species were classified as uncertain despite previous studies identifying them as durophages (e.g., marine stereogenyine podocnemidids; Ferreira et al. 2015); (2) rejections of previous proposals of durophagy (e.g., the thalassochelydian *Sandownia harrisi*; Meylan et al. 2000, Evers and Joyce 2020); (3) proposals of durophagy for species with hitherto unclear feeding ecology (e.g., the protostegid *Rhinochelys pulchriceps*); and (4) confirmations of previous assessments based on comparative osteology (e.g., baenids, pan-cheloniids; Parham and Pyenson 2010; Joyce and Lyson 2015). The predicted evasiveness index for fossils (Fig. 4; Table S11) returns medium-to-high values (0.4–0.7) for stem-turtle clades with proposed freshwater aquatic (paracryptodires, xinjiangchelyids) or marine (thalassochelydians) habits, and medium-to-low values for extinct chelonioids (0.5–0.02), for which our results imply

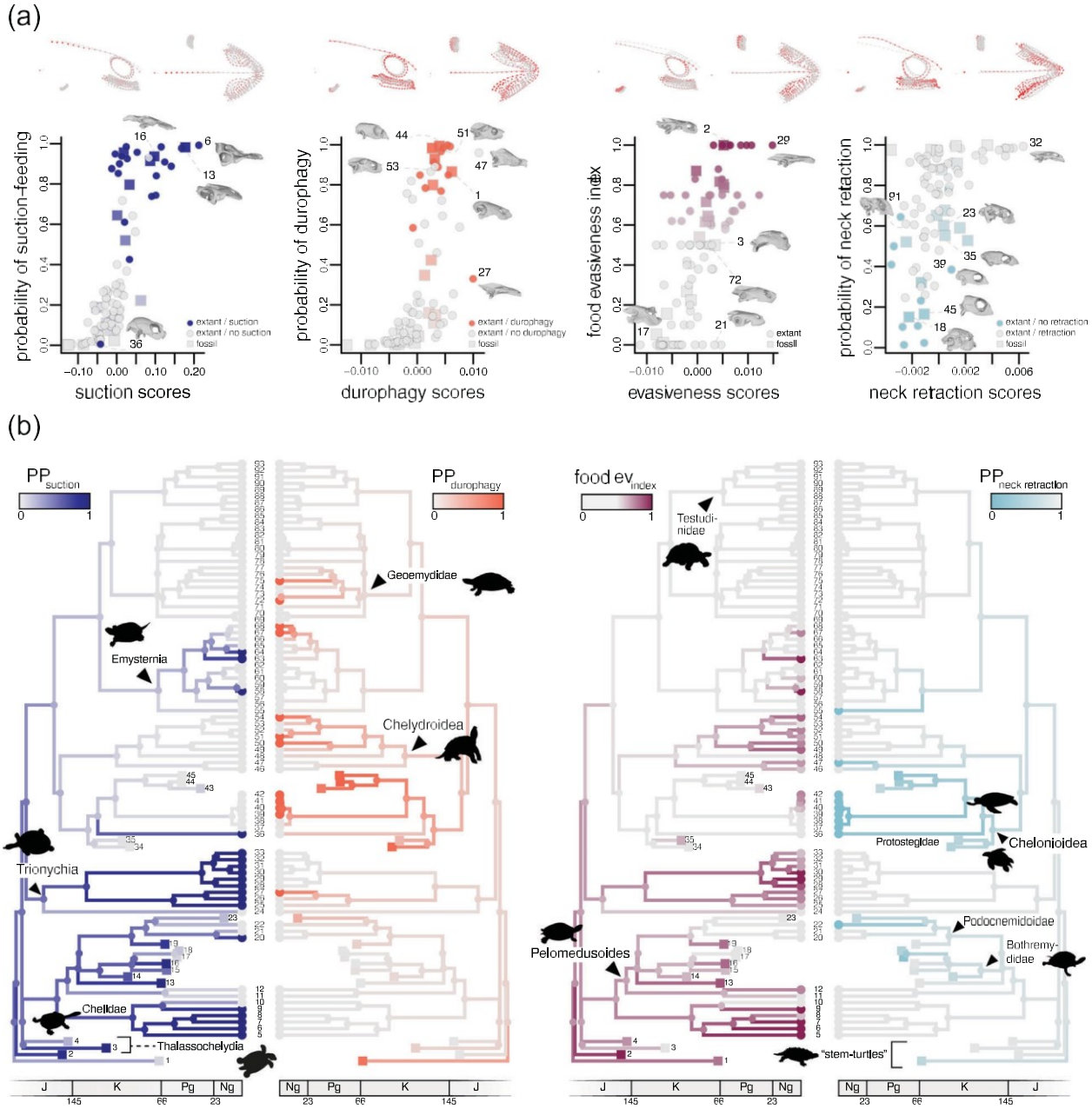

Figure 4. Evolutionary patterns of ecological attributes in extant and fossil turtles. (a) Multivariate regression scores from the best D-PGLS model using the "partial dataset" ($N = 76$) plotted against posterior probabilities of exhibiting a given trait derived from pFDA. Landmark configurations above each plot denote shape deformations (in right lateral and ventral views) associated to each predictor individually. See Figures S18-S22 for alternative plots with vectors indicating the direction of change for each landmark. Selected numbers correspond to *Eubaena cephalica* (1), *Annemys* sp. (2), *Sandownia harrisi* (3), *Chelus fimbriatus* (6), *Sahonachelys mailakavava* (13), *Labrostochelys galkini* (16), *Phosphatochelys tedfordi* (17), *Ummulisani rutgersensis* (18), *Podocnemis expansa* (21), *Bairdemys hartsteini* (23), *Cycloderma frenatum* (27), *Chitra indica* (29), *Pelodiscus sinensis* (32), *Desmatochelys lowii* (35), *Dermochelys coriacea* (36), *Eretmochelys imbricata* (39), *Caretta caretta* (40), *Puppigerus camperi* (44), *Macrochelys temminckii* (47), *Argillochelys antiqua* (45), *Sternotherus minor* (51), *Kinosternon baurii* (53), *Malayemys subtrijuga* (72), and *Aldabrachelys gigantea* (91). See Figure S25 for individually labeled taxa. (b) Posterior probability of presence of each binary trait of the best D-PGLS model ($N = 76$; Table 2) and food evasiveness index mapped onto a time-scaled composite topology based on Evers et al. (2019). Extant species are colored according to presence/absence of a binary trait, whereas fossils are colored according to their PP_{trait}. Numbers correspond to tip labels (see Fig. S7 for entire phylogeny).

durophagy. Predictions for fossil pelomedusoids indicate high feeding disparity, with varied indices ranging from very low (0.1, *Phosphatochelys tedfordi*) to very high in fossil species that were proposed to be suction-feeders (0.84, *Sah. mailakavava*; Joyce et al. 2021b).

Discussion

RELATIONSHIPS OF SKULL SHAPE WITH ECOLOGY AND FUNCTION IN TURTLES

Turtle skulls are strongly modified among reptiles, and characterized by many unusual features (e.g., presence of emarginations, absence of kinesis, teeth, and temporal fenestration). Due to their modified postcranial skeleton (notably the presence of a shell), turtles primarily use the skull for interactions with their environment, including food acquisition, for which neck mobility is a key feature (Pritchard 1984; Herrel et al. 2008; Anquetin et al. 2017a). The evolution of individual anatomical aspects of the turtle skull is well-understood (e.g., fusion of intracranial joints: Rabi et al. 2013). However, the skull ecomorphology is poorly constrained, and functional aspects such as neck retraction have not been included in previous attempts at its understanding (e.g., Claude et al. 2004; Foth et al. 2017).

Our ecomorphological regression models show that ecology only has an effect on turtle skull shape variation (i.e., not on size variation), whereas a key functional variable, the capacity for neck retraction, influences both the relative sizes and shapes of turtle skulls (Tables 1 and 2). No previous study has explicitly tested the allometric relationships of turtle skull size and body size, or the effect of neck retraction or ecological variables on skull size. We find that skull size has strong negative allometry in relation to body size; that is, large-bodied turtles have proportionally smaller heads than small-bodied turtles. The independent effect of neck retraction on this relationship shows that turtles with neck retraction have yet smaller heads, whereas turtles without neck retraction have proportionally larger heads (e.g., *Platysternon megacephalum*; Fig. 2). Neck retraction may therefore impose a limit to maximum relative skull size in turtles. However, ecological traits, such as habitat or diet, have no influence on head size variation in turtles (Table 1).

In contrast, ecological traits do have significant independent effects on turtle skull shape variation, alongside allometry and functional traits. Evolutionary allometry explains 4.45% of skull shape variation (Table 2), similar to previous studies (4%−5.7% in Claude et al. 2004; 5%−7.5% in Foth et al. 2017). The effect of skull size relates primarily to skull length, with large-headed turtles having proportionally short skulls (Figs. 3a, S9). Neck retraction explains an even higher proportion of skull shape variation (4.8%), indicating the importance of neck mobility on skull disparity. Turtles with neck retraction have low, long skulls with deep emarginations, compared to turtles that lack neck retraction, which have high, short skulls with reduced emarginations (Figs. 3a, S13).

Significant ecological predictors explain up to 17% of shape variation and are related to aquatic feeding, and to specific strategies of aquatic feeding, namely, durophagy and food hardness, suction-feeding, and prey elusiveness (Table 2). These results corroborate previous findings of evolutionary changes described for turtles that feed in aquatic environments (e.g., Bramble and Wake 1985; Claude et al. 2004; Lemell et al. 2019). For instance, turtles that feed in the water have dorsoventrally lower skulls with longer posterior processes than terrestrial feeders, which is possibly related to the accommodation of jaw musculature and the use of a generalised suction force to feed under water (Van Damme and Aerts 1997; Claude et al. 2004; Ferreira et al. 2020). They also have flattened rather than vaulted palates, possibly related to a smaller tongue, which plays a minor role in aquatic feeding compared to terrestrial feeding (Bramble and Wake 1985; Winokur 1988; Natchev et al. 2015). We demonstrate that feeding increasingly on harder prey (durophagy and prey hardness) overall correlates with increased head heights (Figs. 3, S14). This may allow a more perpendicular orientation of jaw muscles, enabling higher bite forces and greater bending strength (e.g., Herrel et al. 2002). Durophagy implies further changes in the shape of the palate (Figs. 3a, S12), such as the mediolateral expansion of the triturating surfaces (Claude et al. 2004). However, this can also be present in primarily non-durophagous taxa that feed occasionally on hard food items (e.g., *Batagur baska*, *Kinosternon baurii*; Pritchard 1979; Moll 1980). Suction-feeding turtles have in general elongate and narrow heads, with forward-placed eyes and narrow palates.

An interesting finding of our work is that species lacking neck retraction have cranial morphologies that are generally also inconsistent with suction-feeding (Figs. 3, S11, S13). This supports biomechanical considerations that neck movements are important in facilitating suction-feeding in turtles (Pritchard 1984), as well as empirical data that show that many suction-feeders engage in fast strikes of the craniocervical system toward their prey (e.g., Van Damme and Aerts 1997; Lemell et al. 2002). Our findings are consistent with the hypothesis that high neck mobility in turtles evolved as an adaptation to hunting under water, and was only later co-opted as a protection mechanism (Anquetin et al. 2017a), therefore representing a potential exaptation. Neck retraction may also impose evolutionary constraints on the height and overall size of turtle skulls, as indicated by our results that turtles without neck retraction have relatively larger heads and dorsoventrally higher skulls (Table 1; Figs. 2, 3). The combination of high skulls and no neck retraction may be a morphological complex related to reduction of the capability to feed on elusive prey. This hypothesis is also supported by

empirical evidence from the diets of large headed non-neck retracting turtles (Jones and Seminoff 2013; Sung et al. 2016).

Substantial skull shape variation remains unexplained in our models (78.3%–81.6% residual variation; Table 2). High residual variation is common in ecomorphological analyses using three-dimensional shape data and Procrustes-distance regressions even for structures with strong proposed form-function relationships (e.g., Navalón et al. 2019: bird beaks; Bronzati et al. 2021: archosaur labyrinths). Our phylomorphospace indicates high similarity among closely related species (Fig. 1). This suggests that at least a portion of the unexplained variance can be attributed to shared evolutionary history, or to unanalyzed drivers that themselves show phylogenetic signal (e.g., musculature and soft tissue traits, developmental factors). Further ecological or functional influences not tested here could also be considered in future.

INFERENCES OF THE ECOLOGICAL AND FUNCTIONAL TRAITS OF EXTINCT TURTLES

Paleoecologists have long shown interest in reconstructing ecology from morphology, and the diets or feeding strategies of fossil turtles have often been inferred from qualitative comparisons with extant species (e.g., Archibald and Hutchison 1979; Meylan et al. 2000; Parham and Pyenson 2010; Cadena et al. 2020; Evers and Joyce 2020; Joyce et al. 2021b). Previous quantitative approaches have documented specific feeding adaptations (i.e., durophagy) in specific parts of the skull or for specific turtle clades (e.g., Claude et al. 2004; Ferreira et al. 2015), and also questioned the reliability of skull shape to estimate paleoecology across turtles (Foth et al. 2017). Our analyses contradict this, showing that skull shape is significantly influenced by ecology (Table 2) and that three-dimensional skull shape can indeed predict many aspects of dietary ecology more strongly than expected based on two-dimensional studies (Foth et al. 2017; see Claude et al. 2004 for three-dimensional study of testudinoids). Despite methodological differences between previous and our studies, this effect can at least be partially attributed to using three-dimensional data: although our three-dimensional approach also covers different "sides" of specimens, we recover high correct classification rates for species for which Foth et al. (2017) recovered incoherent results among different two-dimensional skull views. This indicates that complex structures such as crania of vertebrates are better characterized in three dimensions and that two-dimensional analyses of complex shape can lead to misleading ecomorphological results. Our pFDA approach provides high confidence to infer the presence of specific ecological traits, based on the high rates of correctly classifying living suction-feeders (93%) and durophages (88%). Our fossil predictions demonstrate that both these ecologies evolved independently in several lineages. In particular, among extinct groups that independently evolved marine habits, which show parallel ecomorphological adaptations to those of living sea turtles (chelonioids). We identify various traits that evolved convergently in different marine groups, including active hunting, in both stem- and crown-turtles (i.e., thalassochelydians, marine bothremydids), and possibly nearshore grazing in specific extinct pleurodires (i.e., the marine bothremydids *Phosphatochelys tedfordi* and *Ummulisani rutgersensis*).

We infer independent origins of suction-feeding in thalassochelydians (e.g., *Sandownia harrisi*, $PP_{suction}$: 0.92), several pleurodiran lineages (e.g., the bothremydid *Labrostochelys galkini*, $PP_{suction}$: 0.92; the pan-podocnemidid *Sahonachelys mailakavava*, $PP_{suction}$: 0.98), and xinjiangchelyids (*Annemys* sp., $PP_{suction}$: 0.9; Table S7). This supports previous hypotheses of predatory lifestyles for many of these turtles (Gaffney et al. 2006; Rabi et al. 2014; Joyce et al. 2021b), but also contradicts the previous hypotheses of durophagy in *Sandownia harrisi* (Meylan et al. 2000; Evers and Joyce 2020). This is a potentially surprising result, but is also supported by qualitative appraisal: *Sandownia* shares several features with some suction-feeding trionychids (e.g., Fig. 1c [PCA]; Dalrymple 1977; see also Meylan et al. 2000) such as the anteriorly positioned orbits and broad palate (although to a greater extent than seen in trionychids). Furthermore, both the cranial and mandibular triturating surfaces of *Sandownia* are strongly arched (see Evers and Joyce 2020), so that there are no occluding crushing surfaces as usually seen in durophagous turtles such as cheloniids. Ecological inferences of *Sandownia* and other turtles will benefit from further testing using, for instance, combined mandibular and cranial morphology. In general, suction-feeding turtles show two primary skull shapes, each of which evolved multiple times among turtles. These are elongate, narrow, and flat skulls (e.g., *Annemys* sp., *Labrostochelys galkini*, extant trionychids) that contrast with broad, short, and flat skulls, with rounded beaks (e.g., *Sandownia harrisi*, *Sahonachelys mailakavava*, *Chelus fimbriatus*). Interestingly, several of the predicted suction-feeders are secondarily marine species (e.g., *Sandownia harrisi*, *Labrostochelys galkini*), showing that this feeding strategy may have been widespread among marine turtles in the past (see also Bardet et al. [2013] for the extinct chelonioid *Ocepechelon*).

Durophagy is another frequently observed feeding strategy among aquatic turtles, which is commonly inferred for extinct species to explain the evolution of broad triturating surfaces in the palate and mandible (e.g., Gaffney et al. 2006; Parham and Pyenson 2010; Cadena 2015; Ferreira et al. 2015; Foth et al. 2017). Inferences of durophagy have particular importance due to the hypothesized role of durophagy in facilitating selective survival of turtle groups across the K/Pg extinction (e.g., Lyson et al. 2019; Evers and Joyce 2020). Our results show that the presence of an expanded palate alone is insufficient for predicting durophagy in turtles.

The enlargement of the posterodorsal emargination, slight lengthening of the preorbital region, and the posterior displacement of the mandibular condyles should also be considered jointly with the expanded palates as adaptations to durophagy (e.g., Fig. 3a). This is also illustrated by non-durophagous extant groups (e.g., kinosternoids, some chelids; Iverson et al. 1989; Bever 2009) and fossil turtles of various lineages (e.g., thalassochelydians, stereogenyines, bothremydids) that clearly exhibit expanded palates, comparable to those of extant durophagous turtles (Gaffney et al. 2006; Cadena 2015; Ferreira et al. 2015; Evers and Joyce 2020). However, representatives of these extinct groups have low $PP_{durophagy}$ values (*Sandownia harrisi*, $PP_{durophagy}$: 0.17; *Bairdemys hartsteini*, $PP_{durophagy}$: 0.42; *Araiochelys hirayamai*, $PP_{durophagy}$: 0.05). This suggests that previous inferences in those extinct turtles (e.g., Gaffney et al. 2006; Cadena 2015; Ferreira et al. 2015; Evers and Joyce 2020) are likely incorrect, given the high correct classification rate for living durophages in the training set (88%).

Other predictions of durophagy confirm earlier inferences (Joyce and Lyson 2015) among fossil species (e.g., the baenid *Eubaena cephalica*, $PP_{durophagy}$: 0.86; Fig. 4). Our results also do not preclude the possibility that turtles not supported for durophagy could not have had hard food items as part of a mixed diet, as seen in some extant turtles with similar broad palates (e.g., *Apalone ferox*; *Emydura victoriae*; *Kinosternon baurii*; Dalrymple 1977; Pritchard 1979; FitzSimmons et al. 2015). Nevertheless, our approach shows that qualitative intuition can be misleading when interpreting morphology in the absence of statistical context.

Our approach also provides hypothesized diets for fossils that were previously difficult to interpret. An example are the possible diets of high-domed marine bothremydid species, which have skull shapes that are superficially similar to those of extant chelonioids (e.g., Gaffney et al. 2006). Specifically, the predicted evasiveness indices of the robust-skulled *Ummulisani rutgersensis* (0.17) and *Phosphatochelys tedfordi* (0.1) are low, as are their predictions for durophagy (*Ummulisani rutgersensis*: 0; *Phosphatochelys tedfordi*: 0.02), possibly supporting previous assessments of these taxa as being herbivorous (Foth et al. 2017). Our predictions do not explicitly assign them "herbivory," although they are consistent with dietary preferences for softer and sedentary food (Fig. 4), as seen in the extant herbivorous *Chelonia mydas*, but also in other extant chelonioids that feed on slow-moving soft invertebrates, such as *Natator depressus* and *Dermochelys coriacea* (Jones and Seminoff 2013). The recovered feeding modes among large-headed bothremydids previously proposed as marine (e.g., *P. tedfordi*, *U. rutgersensis*) are indeed consistent with a marine ecology, whereas proposed nonmarine bothremydids (e.g., *Galianemys*) are found to have less specialized feeding strategies. We interpret this as tentative evidence that the ecological predictions based on depositional environments were indeed correct for these species.

EVOLUTION OF NECK RETRACTION

Our study allows important new insights into the evolution and functional importance of neck retraction, which were previously poorly understood despite the role of neck mobility in ecological specialization of extant turtles (Pritchard 1984; Herrel et al. 2002; Lemell et al. 2002). Neck retraction is returned as significant in explaining both skull size and shape variation among turtles according to our models (Tables 1 and 2). The presence of neck retraction has profound and comparatively strong effects on turtle skull shape, particularly regarding the emarginations (Fig. 2b,c). In turtles with neck retraction, emarginations are relatively large, and the size of the posterodorsal and anterolateral emarginations is inversely correlated (Fig. 2c; see Werneburg 2015; Ferreira et al. 2020). In contrast, turtles that lack neck retraction have greatly reduced emarginations (Figs. 3a, S13). We propose that the influence of neck retraction on skull shape is stronger in smaller bodied species than in larger ones, because the absence of neck retraction and the evolution of large skulls imply similar gross skull shape changes, particularly cranial shortening (Figs. 3a, S9). In this regard, it is also noteworthy that the largest proportion of neck retraction misclassifications are seen among large headed turtles that retract their necks, but which were predicted to not have that ability (e.g., the Aldabra giant tortoise *Aldabrachelys gigantea*; Fig. 4a).

Our analyses provide higher credibility for predictions of neck retraction than for its absence (Tables S9 and S10), providing constraints on the timing of its origin along the turtle stem-lineage. Although it is already known that the earliest shelled turtles lacked full neck retraction (Gaffney 1975; Werneburg et al. 2015a), the timing of the origin of this key innovation has not been constrained, but is expected to either happen among the extended turtle stem-lineage, which includes several distinct clades (e.g., meiolaniforms, paracryptodires, xinjiangchelyids), or separately in stem-cryptodires and stem-pleurodires (Werneburg et al. 2015a,b). We find that crownward stem-turtles such as xinjiangchelyids (*Annemys* sp., PP_{neck}: 0.98) and thalassochelydians (*Jurassichelon oleronensis*, PP_{neck}: 0.97; *Sandownia harrisi*, PP_{neck}: 1) all retracted their necks, demonstrating that neck retraction was present in stem-turtles by the Late Jurassic. Intermediate posterior probabilities indicate higher uncertainty for paracryptodires (*Eubaena cephalica*, PP_{neck}: 0.58). Our current variable uses the presence versus absence of neck retraction for extant turtles, and as such also only makes "absolute" predictions regarding this feature in turtles. This potential caveat should be addressed in future studies, potentially by quantifying neck mobility as a spectrum of biomechanically possible movements. Our results regarding xinjiangchelyids as

the oldest definitive neck retractors are potentially supported by paleontological evidence, particularly diverse neck morphologies regarding the intercentral articulations (Obraztsova and Danilov 2015; Werneburg et al. 2015b).

Our regression models show that neck retraction, ecology, and skull shape disparity are linked, indicating that neck retraction, as our proxy for neck mobility, plays an important ecomorphological role. Thus, we hypothesize that neck mobility was a key innovation for the ecological diversification of turtles, allowing the evolution of specialized feeding strategies, such as suction-feeding and subaqueous hunting. Although our numerical analyses are inconclusive regarding neck retraction in our sampled paracryptodire (*Eubaena cephalica*), these turtles are thought to have lived in different types of freshwater aquatic habitats (Hutchison 1984; Joyce and Lyson 2015), and their ecological diversity is supported by a wide range of skull morphologies. This includes elongate, narrow, and flat skulls, with moderately deep emarginations (e.g., *Glyptops ornatus*, *Pleurosternon bullockii*; Evans and Kemp 1976; Gaffney 1979; Evers et al. 2020) and short, relatively high skulls, with weak emarginations (e.g., *Uluops uluops*; Carpenter and Bakker 1990; Rollot et al. 2021). Given that we know skull shape correlates with neck retraction in extant turtles (Fig. 3a), and that equally disparate groups such as pelomedusoids show a wide range of predicted values for this trait (Fig. 4b; Table S11), we speculate that neck retraction was variously present among paracryptodires, although this requires formal testing.

Neck retraction was secondarily lost several times independently among crown-group turtles. Three of these cases are individual freshwater species, the chelydroid *Macrochelys temminckii*, the pelomedusoid *Peltocephalus dumerilianus*, and the platysternid *Platysternon megacephalum* (Pritchard 1979; Herrel et al. 2002; Werneburg 2015), all of which have comparatively large heads. Apart from these, neck retraction was secondarily lost mainly among marine turtles, including among extinct bothremydids (e.g., *Phosphatochelys tedfordi*, PP_{neck}: 0.14). Our results also place constraints on the timing of the loss of neck retraction on the stem-lineage of Chelonioidea, the extant sea turtles. The sampled crown-chelonioids (e.g., the Eocene pan-cheloniid *Argillochelys antiqua*, PP_{neck}: 0.23) indicate that the ancestors of crown-chelonioids lacked neck retraction, as in the living species. However, the absence of neck retraction in protostegid stem-chelonioids (e.g., Raselli 2018; Evers et al. 2019; Gentry et al. 2019) is uncertain (e.g., *Desmatochelys lowii*, PP_{neck}: 0.61; *Rhinochelys pulchriceps*, PP_{neck}: 0.64), suggesting that loss of neck retraction may have occurred close to the origin of the chelonioid crown-group.

Our study has implications for ecomorphological studies of complex shapes, such as crania. Combination of allometric, ecological, and functional explanatory variables in multiple regression models allowed us to test specific hypotheses of turtle evolution most of which were previously formulated by qualitative observations—such as the influence of neck retraction on skull size constraints, on temporal emargination shape, and on hunting strategies. These represent different adaptive influences, which can be differentiated and whose independent and significant impact can be assessed by models such as those presented herein. We advocate that studies on various organismal groups should in future formulate models using combined variables that test specific functional or ecological hypotheses. Our analyses also indicate that three-dimensionally captured shape of crania provides coherent correlations of shape aspects with biologically grounded explanatory variables, allowing ecological and functional predictions based on shape. This differs from previous two-dimensional approaches that failed to provide accurate predictions for turtles. Our methodological pipeline requires knowledge of the ecology and function of extant turtles, and therefore underlines the importance of neontological anatomical work and field observations for the study of fossils and organismal evolution.

AUTHOR CONTRIBUTIONS

GH, RBJB, and SWE conceived the study. GH, SWE, and GSF collected data. GH and RBJB wrote code for analyses. GH performed analyses. GH and SWE drafted this article. All authors assisted with editing and reviewing the final version of the text.

ACKNOWLEDGMENTS

GH and SWE were supported by an SNF Ambizione fellowship awarded to SWE (SNF PZ00P2_202019/1). GH was supported by Fundação de Amparo à Pesquisa do Estado de São Paulo (grants 2019/02086-6 and 2019/21787-5). We are thankful to all curators and researchers who provided access to specimens, particularly C. Mehling and M. Norell (AMNH); M. Riley (CAMSM); W. Simpson and A. Resatar (FMNH); A. Folie, U. Lefèvre, and C. Cousin (IRSNB); A. Esguicero and H. F. dos Santos (LIRP); R. C. da Silva (MCT); A. Peaker (MIWG); S. Chapman, P. Barrett, and P. Campbell (NHM London); A. Kupfer (SMNS); and J. Head (UMZC). We also thank research and technical staff at the CT scanning facilities, particularly Y. Hongyu (AMNH, IVPP); F. Ahmed (NHM London); T. Davies (University of Bristol); Z.-X. Luo and A. I. Neander (University of Chicago); and D. Cavalari (University of São Paulo). We also thank researchers who shared CT data with us, namely, W. Joyce, I. Werneburg, D. Brinkman, M. Jones, R. Chatterjee, J. Anquetin, F. Deantoni, and E. Heiss. We also thank the people who have in the past uploaded CT data to online repositories like Digimorph, MorphoSource and MorphoMuseuM, particularly J. Maisano, P. Pritchard, T. Rowe, M. Colbert, G. Watkins-Colwell, Y. Rollot, and A.-K. Mautner. W. Joyce, T. Kohlsdorf, S. Onary-Alves, P. Rizzato, J. F. Rodrigues, and F. Souza are thanked for extended discussion of preliminary results, and D. Adams, M. Collyer, and L. Schmitz for discussion on phylogenetic comparative methods. Lastly, we want to thank M. Zelditch, R. Warnock, T. Guillerme, and an anonymous reviewer for their insightful comments that helped improved the manuscript.

Open access funding provided by CSAL.

CONFLICT OF INTEREST

The authors declare no conflict of interest.

DATA ARCHIVING

All CT data collected by us for this study were deposited in the online repository MorphoSource, in which scans have unique Media IDs. Media IDs and availability information for scans shared with us are outlined in detail in Text S1. All three-dimensional models created in this study and used for landmarking are deposited in a MorphoSource collection (Project ID 000398451; https://www.morphosource.org/projects/000398451), with models linked to their parent CT data. Landmark data, phylogenetic trees, and R code to reproduce our statistical analyses are published in GitHub (https://github.com/G-Hermanson/Turtle-cranial-ecomorphology). An archived version of code and data is also available at Zenodo (https://doi.org/10.5281/zenodo.7018313). All other supporting data are included in Supporting Information S1 and S2.

REFERENCES

Adams, D.C. (2014) A method for assessing phylogenetic least squares models for shape and other high-dimensional multivariate data. *Evolution*, 68, 2675–2688.

Adams, D.C. & Collyer, M.L. (2018a) Phylogenetic ANOVA: group-clade aggregation, biological challenges, and a refined permutation procedure. *Evolution*, 72, 1204–1215.

——— (2018b) Multivariate phylogenetic comparative methods: evaluations, comparisons, and recommendations. *Syst. Biol.*, 67, 14–31.

Adams, D.C. & Felice, R.N. (2014) Assessing trait covariation and morphological integration on phylogenies using evolutionary covariance matrices. *PLoS ONE*, 9, e94335.

Adams, D.C., Collyer, M.L. & Kaliontzopoulou, A. (2020) Geomorph: software for geometric morphometric analyses. R package version 3.2.1. Available via https://cran.r-project.org/package=geomorph.

Alcaldade, L., Derocco, N.N. & Rosset, S.D. (2010) Feeding in syntopy: diet of *Hydromedusa tectifera* and *Phrynops hilarii* (Chelidae). *Chelonian Conservation and Biology*, 9, 33-44.

Anquetin, J., Barrett, P.M., Jones, M.E.H., Moore-Fay, S. & Evans, S.E. (2009) A new stem turtle from the Middle Jurassic of Scotland: new insights into the evolution of palaeoecology of basal turtles. *Proceedings of the Royal Society B: Biological Sciences*, 276, 879–886.

Anquetin, J., Püntener, C. & Joyce, W.G. (2017b) A review of the fossil record of turtles of the clade Thalassochelydia. *Bulletin of the Peabody Museum of Natural History*, 58, 317–369.

Anquetin, J., Tong, H. & Claude, J. (2017a) A Jurassic stem pleurodire sheds light on the functional origin of neck retraction in turtles. *Scientific Reports*, 7, 1–10.

Archibald, J.D. & Hutchison, J.H. (1979) Revision of the genus *Palatobaena* (Testudines, Baenidae) with the description of a new species. *Postilla*, 177, 1–19.

Bardet, N., Jalil, N.E., de Lapparent de Broin, F., Germain, D., Lambert, O. & Amaghzaz, M. (2013) A giant chelonioid turtle from the Late Cretaceous of Morocco with a suction feeding apparatus unique among tetrapods. *PloS one*, 8, e63586.

Bardua, C., Felice, R.N., Watanabe, A., Fabre, A.C. & Goswami, A. (2019) A practical guide to sliding and surface semilandmarks in morphometric analyses. *Integrative Organismal Biology*, 1, obz016.

Bels, V.L., Davenport, J. & Renous, S. (1998) Food ingestion in the estuarine turtle *Malaclemys terrapin*: comparison with the marine leatherback turtle *Dermochelys coriacea*. *Journal of the Marine Biological Association of the United Kingdom*, 78, 953–972.

Benjamin, Y. & Hochberg, Y. (1995) Controlling the false discovery rate: a practical and powerful approach to multiple testing. *Journal of the Royal Statistical Society: Series B (Methodological)*, 57, 289–300.

Bever, G.S. (2009) Postnatal ontogeny of the skull in the extant North American turtle *Sternotherus odoratus* (Cryptodira: Kinosternidae). *Bulletin of the American Museum of Natural History*, 330, 1–97.

Bever, G.S., Lyson, T.R., Field, D.J. & Bhullar, B.A.S. (2015) Evolutionary origin of the turtle skull. *Nature*, 525, 239–242.

Bookstein, F.L. (1991) Thin-plate splines and the atlas problem for biomedical images. Pp. 326–342 *in* A. C. F. Colchester and D. J. Hawkes, eds. Biennial International Conference on Information Processing in Medical Imaging. Springer, Berlin.

Bramble, D.M. & Wake, D.B. (1985) Feeding mechanisms of lower tetrapods. In Functional vertebrate morphology (eds. M., Hildebrand, D. M., Bramble, K. F., Liem & D. B., Wake), 230–261. Univ. of Chicago Press, Chicago.

Bronzati, M., Benson, R.B.J., Evers, S.W., Ezcurra, M.D., Cabreira, S.F., Choiniere, J., Dollman, K.N., Paulina-Carabajal, A., Radermacher, V.J., da Silva, L.R., et al (2021) Deep evolutionary diversification of semicircular canals in archosaurs. *Current Biology*, 31, 2520–2529.

Burnham, K.P. & Anderson, D.R. (2002) Model selection and multimodel inference: a practical information-theoretic approach. Springer, Berlin.

Cadena, E. (2015) The first South American sandownid turtle from the Lower Cretaceous of Colombia. *PeerJ*, 3, e1431. https://doi.org/10.7717/peerj.1431.

Cadena, E.A., Scheyer, T.M., Carrillo-Briceño, J.D., Sánchez, R., Aguilera-Socorro, O.A., Vanegas, A., Pardo, M., Hansen, D.M. & Sánchez-Villagra, M.R. (2020) The anatomy, paleobiology, and evolutionary relationships of the largest extinct side-necked turtle. *Science Advances*, 6, eaay4593. https://doi.org/10.1126/sciadv.aay4593.

Carpenter, K. & Bakker, R.T. (1990) A new latest Jurassic vertebrate fauna, from the highest levels of the Morrison Formation at Como Bluff, Wyoming, with comments on Morrison biochronology. Part II. A new baenid turtle. *Hunteria*, 2, 3–4.

Chapelle, K.E.J., Benson, R.B.J., Stiegler, J., Otero, A., Zhao, Q. & Choiniere, J.N. (2020) A quantitative method for inferring locomotory shifts in amniotes during ontogeny, its application to dinosaurs and its bearing on the evolution of posture. *Palaeontology*, 63, 229–242.

Claude, J., Paradis, E., Tong, H. & Auffray, J.C. (2003) A geometric morphometric assessment of the effects of environment and cladogenesis on the evolution of the turtle shell. *Biological Journal of the Linnean Society*, 79, 485–501.

Claude, J., Pritchard, P.C.H., Tong, H., Paradis, E. & Auffray, J.C. (2004) Ecological correlates and evolutionary divergence in the skull of turtles: a geometric morphometric assessment. *Systematic Biology*, 53, 933–948.

Clavel, J., Aristide, L. & Morlon, H. (2019) A penalized likelihood framework for high-dimensional phylogenetic comparative methods and an application to new-world monkeys brain evolution. *Systematic Biology*, 68, 93–116.

Crawford, N.G., Faircloth, B.C., McCormack, J.E., Brumfield, R.T., Winker, K. & Glenn, T. (2012) More than 1000 ultraconserved elements provide evidence that turtles are the sister group of archosaurs. *Biology Letters*, 8, 783–786.

Dalrymple, G.H. (1977) Intraspecific variation in the cranial feeding mechanism of turtles of the genus *Trionyx* (Reptilia, Testudines, Trionychidae). *Journal of Herpetology*, 11, 255–285.

——— (1979) Packaging problems of head retraction in trionychid turtles. *Copeia*, 1979, 655–660.

Drake, A.G. & Klingenberg, C.P. (2008) The pace of morphological change: historical transformation of skull shape in St Bernard dogs. *Proceedings of the Royal Society B: Biological Sciences*, 275, 71–76.

Dziomber, L., Joyce, W.G. & Foth, C. (2020) The ecomorphology of the shell of extant turtles and its applications for fossil turtles. *PeerJ*, 8, e10490. https://doi.org/10.7717/peerj.10490.

Ernst, C.H. & Barbour, R.W. (1989) Turtles of the world. Smithsonian Institution Press, Washington, D.C.

Evans, J. & Kemp, T.S. (1976) A new turtle skull from the Purbeckian of England and a note on the early dichotomies of cryptodire turtles. *Palaeontology*, 19, 317–324.

Evers, S.W. & Benson, R.B.J. (2019) A new phylogenetic hypothesis of turtles with implications for the timing and number of evolutionary transitions to marine lifestyles in the group. *Palaeontology*, 62, 93–134.

Evers, S.W. & Joyce, W.G. (2020) A re-description of *Sandownia harrisi* (Testudinata: Sandownidae) from the Aptian of the Isle of Wight based on computed tomography scans. *Royal Society Open Science*, 7, 191936.

Evers, S.W., Barrett, P.M. & Benson, R.B.J. (2019) Anatomy of *Rhinochelys pulchriceps* (Protostegidae) and marine adaptation during the early evolution of chelonioids. *PeerJ*, 7, e6811.

Evers, S.W., Rollot, Y. & Joyce, W.G. (2020) Cranial osteology of the Early Cretaceous turtle *Pleurosternon bullockii* (Paracryptodira: Pleurosternidae). *PeerJ*, 8, e9454.

Felsenstein, J. (1985) Phylogenies and the comparative method. *The American Naturalist*, 125, 1–15.

Ferreira, G.S., Rincon, A.D., Solórzano, A. & Langer, M.C. (2015) The last marine pelomedusoids (*Testudines*: *Pleurodira*): a new species of *Bairdemys* and the paleoecology of *Stereogenyina*. *PeerJ*, 3, e1063.

Ferreira, G.S., Lautenschlager, S., Evers, S.W., Pfaff, C., Kriwet, J., Raselli, I. & Werneburg, I. (2020) Feeding biomechanics suggests progressive correlation of skull architecture and neck evolution in turtles. *Scientific Reports*, 10, 1–11.

Field, D.J., Gauthier, J.A., King, B.L., Pisani, D., Lyson, T.R. & Peterson, K.J. (2014) Toward consilience in reptile phylogeny: miRNAs support archosaur, not lepidosaur, affinity for turtles. *Evolution & Development*, 16, 189–196.

FitzSimmons, N.N., Featherston, P. & Tucker, A.D. (2015) Comparative dietary ecology of turtles (*Chelodina burrungandjii* and *Emydura victoriae*) across the Kimberley Plateau, Western Australia, prior to the arrival of cane toads. *Marine and Freshwater Research*, 67, 1611-1624.

Foth, C., Rabi, M. & Joyce, W.G. (2017) Skull shape variation in extant and extinct Testudinata and its relation to habitat and feeding ecology. *Acta Zoologica*, 98, 310–325.

Foth, C., Evers, S.W., Joyce, W.G., Volpato, V.G. & Benson, R.B.J. (2019) Comparative analysis of the shape and size of the middle ear of turtles reveals no correlation with habitat ecology. *Journal of Anatomy*, 235, 1078-1097.

Gaffney, E.S. (1972) The systematics of the North American family Baenidae (Reptilia, Cryptodira). *Bulletin of the American Museum of Natural History*, 147, 241–320.

——— (1975) A phylogeny and classification of the higher categories of turtles. *Bulletin of the American Museum of Natural History*, 155, 387–436.

——— (1979) Comparative cranial morphology of Recent and fossil turtles. *Bulletin of the American Museum of Natural History*, 164, 67–376.

——— (1990) The comparative osteology of the Triassic turtle *Proganochelys*. *Bulletin of the American Museum of Natural History*, 194, 1–263.

Gaffney, E.S., Tong, H. & Meylan, P.A. (2006) Evolution of the side-necked turtles: the families Bothremydidae, Euraxemydidae, and Araripemydidae. *Bulletin of the American Museum of Natural History*, 300, 1–698.

Gaffney, E.S., Meylan, P.A., Wood, R.C., Simons, E. & Campos, D.A. (2011) Evolution of the side-necked turtles: the family Podocnemididae. *Bulletin of the American Museum of Natural History*, 350, 1–237.

Gentry, A.D., Ebersole, J.A. & Kiernan, C.R. (2019) *Asmodochelys parhami*, a new fossil marine turtle from the Campanian Demopolis Chalk and the stratigraphic congruence of competing marine turtle phylogenies. *Royal Society Open Science*, 6, 191950.

Godoy, P.L. (2020) Crocodylomorph cranial shape evolution and its relationship with body size and ecology. *Journal of Evolutionary Biology*, 33, 4–21.

Gower, J.C. (1975) Generalized Procrustes analysis. *Psychometrika*, 40, 33–51.

Grafen, A. (1989) The phylogenetic regression. *Philosophical Transactions of the Royal Society of London. B, Biological Sciences*, 326, 119–157.

Guillerme, T., Weisbecker, V. & Marcy, A. (2021) landvR: tools for measuring landmark position variation. R package version 0.5.2. Available via https://github.com/TGuillerme/landvR.

Gunz, P. & Mitteroecker, P. (2013) Semilandmarks: a method for quantifying curves and surfaces. *Hystrix, the Italian Journal of Mammalogy*, 24, 103–109.

Hermanson, G. (2021) Data and annotated R scripts associated with "Cranial ecomorphology of turtles and neck retraction as a possible trigger of ecological diversification. *GitHub*, https://github.com/G-Hermanson/Turtle-cranial-ecomorphology.

Herrel, A., O'Reilly, J.C. & Richmond, A.M. (2002) Evolution of bite performance in turtles. *Journal of Evolutionary Biology*, 15, 1083–1094.

Herrel, A., Van Damme, J. & Aerts, P. (2008) Cervical Anatomy and Function in Turtles. In Biology of turtles (eds. J., Wyneken, M. H., Godfrey & V., Bels), 163–185. CRC Press, Boca Raton, FL.

Hirayama, R. (1998) Oldest known sea turtle. *Nature*, 392, 705–708.

Ho, L.S.T. & Ané, C. (2014) A linear-time algorithm for Gaussian and non-Gaussian trait evolution models. *Systematic Biology*, 63, 397–408.

Hutchison, J.H. (1984) Determinate growth in the Baenidae (Testudines): taxonomic, ecologic, and stratigraphic significance. *Journal of Vertebrate Paleontology*, 3, 148–151.

Iverson, J.B., Ernst, C.H., Gotte, S. & Lovich, J.E. (1989) The validity of *Chinemys megalocephala* (Testudines: Batagurinae). *Copeia*, 1989, 494–498.

Ives, A.R. (2019) R^2s for correlated data: phylogenetic models, LMMs, and GLMMs. *Systematic Biology*, 68, 234–251.

Jafari, M. & Ansari-Pour, N. (2019) Why, when and how to adjust your P values? *Cell Journal (Yakhteh)*, 20, 604–607.

Jetz, W., Thomas, G.H., Joy, J.B., Hartmann, K. & Mooers, A.O. (2012) The global diversity of birds in space and time. *Nature*, 491, 444–448.

Jones, T.T. & Seminoff, J.A. (2013) Feeding biology: advances from field-based observations, physiological studies, and molecular techniques. In The biology of sea turtles (eds. J., Wyneken, K. J., Lohmann & J. A., Musick), 211–247. CRC Press.

Joyce, W.G. (2015) The origins of turtles: a paleontological perspective. *Journal of Experimental Zoology Part B: Molecular and Developmental Evolution*, 324, 181–193.

——— (2017) A review of the fossil record of basal Mesozoic turtles. *Bulletin of the Peabody Museum of Natural History*, 58, 65–113.

Joyce, W.G. & Gauthier, J.A. (2004) Palaeoecology of Triassic stem turtles sheds new light on turtle origins. *Proceedings of the Royal Society of London. Series B: Biological Sciences*, 271, 1–5.

Joyce, W.G. & Lyson, T.R. (2015) A review of the fossil record of turtles of the clade Baenidae. *Bulletin of the Peabody Museum of Natural History*, 56, 147–183.

Joyce, W.G., Mäuser, M. & Evers, S.W. (2021a) Two turtles with soft tissue preservation from the platy limestones of Germany provide evidence for marine flipper adaptations in Late Jurassic thalassochelydians. *PloS one*, 16, e0252355.

Joyce, W.G., Rollot, Y., Evers, S.W., Lyson, T.R., Rahantarisoa, L.J. & Krause, D.W. (2021b) A new pelomedusoid turtle, *Sahonachelys mailakavava*, from the Late Cretaceous of Madagascar provides evidence for convergent evolution of specialized suction feeding among pleurodires. *Royal Society Open Science*, 8, 210098.

Kammerer, C.F., Deutsch, M., Lungmus, J.K. & Angielczyk, K.D. (2020) Effects of taphonomic deformation on geometric morphometric analysis of fossils: a study using the dicynodont *Diictodon feliceps* (Therapsida, Anomodontia). *PeerJ*, 8, e9925.

Law, C.J., Duran, E., Hung, N., Richards, E., Santillan, I. & Mehta, R.S. (2018) Effects of diet on cranial morphology and biting ability in musteloid mammals. *Journal of Evolutionary Biology*, 31, 1918–1931.

Lemell, P., Lemell, C., Snelderwaard, P., Gumpenberger, M., Wochesländer, R. & Weisgram, J. (2002) Feeding patterns of *Chelus fimbriatus* (Pleurodira: Chelidae). *The Journal of Experimental Biology*, 205, 1495–1506.

Lemell, P., Natchev, N., Beisser, C.J. & Heiss, E. (2019) Feeding in turtles: understanding terrestrial and aquatic feeding in a diverse but monophyletic group. In Feeding in vertebrates (eds. V., Bels & I. Q., Whishaw), 611–642. Springer Nature Switzerland AG, Cham, Switzerland.

Li, C., Wu, X.C., Rieppel, O., Wang, L.T. & Zhao, L.J. (2008) An ancestral turtle from the Late Triassic of China. *Nature*, 456, 497–501.

Lowi-Merri, T.M., Benson, R.B.J., Claramunt, S. & Evans, D.C. (2021) The relationship between sternum variation and mode of locomotion in birds. *BMC Biology*, 19, 1–23.

Lyson, T.R., Rubidge, B.S., Scheyer, T.M., de Queiroz, K., Schachner, E.R., Smith, R.M.H., Botha-Brink, J. & Bever, G.S. (2016) Fossorial origin of the turtle shell. *Current Biology*, 26, 1887–1894.

Lyson, T.R., Miller, I.M., Bercovici, A.D., Weissenburger, K., Fuentes, A.J., Clyde, W.C., Hagadorn, J.W., Butrim, M.J., Johnson, K.R., Fleming, R.F., et al (2019) Exceptional continental record of biotic recovery after the Cretaceous-Paleogene mass extinction. *Science (New York, N.Y.)*, 366, 977–983.

Marek, R.D., Falkingham, P.L., Benson, R.B.J., Gardiner, J.D., Maddox, T.W. & Bates, K.T. (2021) Evolutionary versatility of the avian neck. *Proceedings of the Royal Society B*, 288, 20203150.

Matzke, A.T., Maisch, M.W., Ge, S., Pfretzschner, H.-U. & Stöhr, H. (2004) A new xinjiangchelyid turtle (Testudines, Eucryptodira) from the Jurassic Qigu Formation of the Southern Junggar Basin, Xinjiang, North-West China. *Palaeontology*, 47, 1267–1299.

Mazerolle, M.J. (2020) AICcmodavg: model selection and multimodel inference based on (Q)AIC(c). R package version 2.3-1. Available via https://cran.r-project.org/package=AICcmodavg.

Meylan, P.A., Moody, R.T., Walker, C.A. & Chapman, S.D. (2000) *Sandownia harrisi*, a highly derived trionychoid turtle (Testudines: Cryptodira) from the Early Cretaceous of the Isle of Wight, England. *Journal of Vertebrate Paleontology*, 20, 522–532.

Moll, E.O. (1980) Natural history of the river terrapin, *Batagur baska* (Gray) in Malaysia (Testudines: Emydidae). *Malaysian Journal of Science*, 6, 23–62.

Motani, R. & Schmitz, L. (2011) Phylogenetic versus functional signals in the evolution of form–function relationships in terrestrial vision. *Evolution: International Journal of Organic Evolution*, 65, 2245–2257.

Natchev, N., Tzankov, N., Werneburg, I. & Heiss, E. (2015) Feeding behaviour in a 'basal' tortoise provides insights on the transitional feeding mode at the dawn of modern land turtle evolution. *PeerJ*, 3, e1172.

Navalón, G., Bright, J.A., Marugán-Lobón, J. & Rayfield, E.J. (2019) The evolutionary relationship among beak shape, mechanical advantage, and feeding ecology in modern birds. *Evolution; International Journal of Organic Evolution*, 73, 422–435.

Nishizawa, H., Asahara, M., Kamezaki, N. & Arai, N. (2010) Differences in the skull morphology between juvenile and adult green turtles: implications for the ontogenetic diet shift. *Current Herpetology*, 29, 97–101.

Obraztsova, E. & Danilov, I. (2015) Morphology of the cervical vertebrae of *Annemys* and variability of neck morphotypes in xinjiangchelyid turtles. *PeerJ PrePrints*, 3, e1088v1. https://doi.org/10.7287/peerj.preprints.1088v1.

Pagel, M. (1999) Inferring the historical patterns of biological evolution. *Nature*, 401, 877–884.

Paradis, E. & Schliep, K. (2019) ape 5.0: an environment for modern phylogenetics and evolutionary analyses in R. *Bioinformatics (Oxford, England)*, 35, 526–528.

Parham, J.F. & Pyenson, N.D. (2010) New sea turtle from the Miocene of Peru and the iterative evolution of feeding ecomorphologies since the Cretaceous. *Journal of Paleontology*, 84, 231–247.

Pereira, A.G., Sterli, J., Moreira, F.R. & Schrago, C.G. (2017) Multilocus phylogeny and statistical biogeography clarify the evolutionary history of major lineages of turtles. *Molecular Phylogenetics and Evolution*, 113, 59–66.

Pincheira-Donoso, D., Bauer, A.M., Meiri, S. & Uetz, P. (2013) Global taxonomic diversity of living reptiles. *PloS one*, 8, e59741.

Pinheiro, J., Bates, D., DebRoy, S. & Sarkar, D. (2020) nlme: linear and nonlinear mixed effects models. R package version 3.1-148. Available via https://CRAN.R-project.org/package=nlme.

Pritchard, P.C.H. (1979) Encyclopedia of turtles. TFH Publications, Inc. Ltd, Neptune City, NJ.

——— (1984) Piscivory in turtles, and evolution of the long-necked Chelidae. In The structure, development and evolution of reptiles (Symposia of the Zoological Society of London) (ed. M. W. J., Ferguson), 87–110. Academic Press, Lond.

R Core Team (2020) R: a language and environment for statistical computing. R Foundation for Statistical Computing, Vienna. https://www.R-project.org/.

Rabi, M., Zhou, C.F., Wings, O., Ge, S. & Joyce, W.G. (2013) A new xinjiangchelyid turtle from the Middle Jurassic of Xinjiang, China and the evolution of the basipterygoid process in Mesozoic turtles. *BMC Evolutionary Biology*, 13, 1–29.

Rabi, M., Sukhanov, V.B., Egorova, V.N., Danilov, I. & Joyce, W.G. (2014) Osteology, relationships, and ecology of *Annemys* (Testudines, Eucryptodira) from the Late Jurassic of Shar Teg, Mongolia, and phylogenetic definitions for Xinjiangchelyidae, Sinemydidae, and Macrobaenidae. *Journal of Vertebrate Paleontology*, 34, 327–352.

Raselli, I. (2018) Comparative cranial morphology of the Late Cretaceous protostegid sea turtle *Desmatochelys lowii*. *PeerJ*, 6, e5964.

Revell, L.J. (2012) phytools: an R package for phylogenetic comparative biology (and other things). *Methods in Ecology and Evolution*, 3, 217–223.

Turtle Taxonomy Working Group, Rhodin, A.G.J., Iverson, J.B., Bour, R., Fritz, U., Georges, A., Shaffer, H.B. & van Dijk, P.P. (2021) Turtles of the world: annotated checklist of taxonomy, synonymy, distribution, and conservation status. 9th ed. Chelonian Research Foundation and Turtle Conservancy, Lunenburg, MA.

Rieppel, O. & Reisz, R.R. (1999) The origin and early evolution of turtles. *Annual Review of Ecology and Systematics*, 30, 1–22.

Rohlf, F.J. & Corti, M. (2000) Use of two-block partial least-squares to study covariation in shape. *Systematic Biology*, 49, 740–753.

Rollot, Y., Evers, S.W. & Joyce, W.G. (2021) A redescription of the Late Jurassic (Tithonian) turtle *Uluops uluops* and a new phylogenetic hypothesis of Paracryptodira. *Swiss Journal of Palaeontology*, 140, 1–30.

Rougier, G.W., de la Fuente, M.S. & Arcucci, A.B. (1995) Late Triassic turtles from South America. *Science (New York, N.Y.)*, 268, 855–858.

Scheyer, T.M. & Sander, P.M. (2007) Shell bone histology indicates terrestrial palaeoecology of basal turtles. *Proceedings of the Royal Society B: Biological Sciences*, 274(1620), 1885–1893.

Schlager, S. (2017) Morpho and Rvcg – shape analysis in R. In Statistical shape and deformation analysis (eds. G., Zheng, S., Li & G., Szekely), 217–256. Academic Press, Cambridge, MA.

Schoch, R.R. & Sues, H.D. (2015) A Middle Triassic stem-turtle and the evolution of the turtle body plan. *Nature*, 523, 584–587.

Schoch, R.R., Klein, N., Scheyer, T.M. & Sues, H.D. (2019) Microanatomy of the stem-turtle *Pappochelys rosinae* indicates a predominantly fossorial mode of life and clarifies early steps in the evolution of the shell. *Scientific Reports*, 9, 1–10.

Sterli, J. (2008) A new, nearly complete stem turtle from the Jurassic of South America with implications for turtle evolution. *Biology Letters*, 4, 286–289.

——— (2015) A review of the fossil record of Gondwanan turtles of the clade Meiolaniformes. *Bulletin of the Peabody Museum of Natural History*, 56, 21–45.

Sterli, J., de la Fuente, M.S. & Rougier, G.W. (2018) New remains of *Condorchelys antiqua* (Testudinata) from the Early-Middle Jurassic of Patagonia: anatomy, phylogeny, and paedomorphosis in the early evolution of turtles. *Journal of Vertebrate Paleontology*, 38, 1–17.

Sugiura, N. (1978) Further analysis of the data by Akaike's information criterion and the finite corrections. *Communications in Statistics - Theory and Methods*, 7, 13–26.

Sung, Y.H., Hau, B.C. & Karraker, N.E. (2016) Diet of the endangered bigheaded turtle *Platysternon megacephalum*. *PeerJ*, 4, e2784.

Van Damme, J. & Aerts, P. (1997) Kinematics and functional morphology of aquatic feeding in Australian snake-necked turtles (Pleurodira; Chelodina). *Journal of Morphology*, 233, 113–125.

Vanhooydonck, B., Herrel, A. & Van Damme, R. (2007) Interactions between habitat use, behavior, and the trophic niche of lacertid lizards. In Lizard ecology: the evolutionary consequences of foraging mode (eds. S. M., Reilly, L. D., McBrayer & D. B., Miles), 427–449. Cambridge Univ. Press, Cambridge, U.K.

Webster, M. & Sheets, H.D. (2010) A practical introduction to landmark-based geometric morphometrics. In Quantitative methods in paleobiology (eds. J., Alroy & G., Hunt), 163–188. The Paleontological Society, Baltimore, MD.

Werneburg, I. (2015) Neck motion in turtles and its relation to the shape of the temporal emargination. *Comptes Rendus Palevol*, 14, 527–548.

Werneburg, I., Hinz, J.K., Gumpenberger, M., Volpato, V., Natchev, N. & Joyce, W.G. (2015a) Modeling neck mobility in fossil turtles. *Journal of Experimental Zoology Part B: Molecular and Developmental Evolution*, 324, 230–243.

Werneburg, I., Wilson, L.A.B., Parr, W.C. & Joyce, W.G. (2015b) Evolution of neck vertebral shape and neck retraction at the transition to modern turtles: an integrated geometric morphometric approach. *Systematic Biology*, 64, 187–204.

Winokur, R.M. (1988) The buccopharyngeal mucosa of the turtles (Testudines). *Journal of Morphology*, 196, 33–52.

Yeh, H.K. (1966) A new Cretaceous turtle of Nanhsiung, northern Kwangtung. *Vertebrata Palasiatica*, 10, 191–200.

Associate Editor: R. Warnock
Handling Editor: M.L. Zelditch

Supporting Information

Additional supporting information may be found online in the Supporting Information section at the end of the article.

Supplementary Information Tables
Supplementary Information Tables